Electronic Supplementary Information

1. Experimental Methods

Materials

Bis(4-bromophenyl)amine (NPh_2), 4,7-dibromobenzo[c]-1,2,5-thiadiazole (BT), 2,7-dibromo-9H-carbazole (CB), tetrakis(triphenylphosphine) palladium(0) (99%), potassium carbonate (K_2CO_3), Span® 80 nonionic surfactant, chloroform-d ($CDCl_3$, 99.8%), methyl phenyl sulfide, dimethylaminopyridine (DMAP) and all other solvents were purchased from Aldrich. 1,3,5-Tribromobenzene and di-tert-butyl dicarbonate (di-Boc) were obtained from Alfa Aesar and 1,3,5-Phenyltriboronic acid (PB) (98%) was purchased from Combi-Blocks Inc. All chemicals and solvents were used as received unless otherwise specified.

Synthesis of Boc-NPh_2

0.991 g NPh_2 (3.05 mmol), 1.334 g di-Boc (6.11 mmol) and 0.373 g DMAP (3.05 mmol) were dissolved in 50 mL dried THF. The reaction mixture was stirred at room temperature under nitrogen for 12 h. After completion, the reaction mixture was poured into 500 mL of Milli-Q water. The precipitate was then washed with cold methanol and dried under vacuum, yielding 1.15 g (89%) product.

^{1}H NMR (Figure S1): 7.35 (d, 2H), 6.98 (d, 2H), 1.37 (s, 9H)

13C NMR (Figure S2): 153.1, 141.7, 131.9, 128.5, 119.3, 82.0, 28.2

FTIR (Figure S5)

Synthesis of Boc-CB

0.991 g CB (3.06 mmol), 1.334 g di-BOC (6.11 mmol) and 0.373 g DMAP (3.05 mmol) were dissolved in 50 mL dried THF. The reaction mixture was stirred at room temperature under nitrogen for 12 h. After completion, the reaction mixture was poured into 500 mL of Milli-Q water. The precipitate was then washed with cold methanol and dried under vacuum, yielding 1.18 g (91%) product.

^{1}H NMR (Figure S3): 8.37 (d, 2H), 7.64 (d, 2H), 7.37 (d, 2H), 1.69 (s, 9H)

13C NMR (Figure S4): 150.3, 139.1, 126.5, 123.8, 121.0, 120.5, 119.6, 85.2, 28.3

FTIR (Figure S6)

General procedure for the Suzuki-Miyaura cross-coupling reactions via high internal phase emulsion HIPE polymerization

To 1 equivalent of PB, 1.5 equivalent of bromo-compound, 5 mol% of tetrakis(triphenylphosphine) palladium(0) and 100 mg of Span® 80 were dissolved in 1 mL of toluene. 6 equivalent of K_2CO_3 was dissolved in 9 mL of Milli-Q water. Then, the aqueous phase was slowly added to the organic phase under vigorous stirring using an Ultra Turrax® IKA T18 mechanical stirrer at 14000 RPM. After 30 min, the homogeneous mixture became viscous and was heated to 80 ^{o}C for 12 h. The resulted polyHIPE was then rinsed with Milli-Q water several times and extracted with 50/50 dichloromethane and methanol solution in a soxhlet for 24 h. Drying of the polyHIPE was then performed using supercritical CO_2 on a CPD 300 critical point dryer.

Synthesis of B-(Boc-NPh$_2$)$_3$

The standard procedure for the Suzuki reaction via HIPE polymerization as mentioned above is applied. 100 mg (0.22 mmol) of PB, 136 mg (0.32 mmol) of NPh, 13 mg (0.011 mmol) tetrakis(triphenylphosphine) palladium(0) and 182 mg (1.32 mmol) K_2CO_3 were used. The yield was 92% (217 mg).

Synthesis of B-(Boc-CB)$_3$

The standard procedure for the Suzuki reaction via HIPE polymerization as mentioned above is applied. 100 mg (0.22 mmol) of PB, 136 mg (0.32 mmol) of CB, 13 mg (0.011 mmol) tetrakis(triphenylphosphine) palladium(0) and 182 mg (1.32 mmol) K_2CO_3 were used. The yield was 83% (195 mg).

Synthesis of B-(Boc-CB)$_{2}$-BT

The standard procedure for the Suzuki reaction via HIPE polymerization as mentioned above is applied. 100 mg (0.22 mmol) of PB, 94 mg (0.22 mmol) of CB, 32 mg (0.11 mmol) of BT, 13 mg (0.011 mmol) tetrakis(triphenylphosphine) palladium(0) and 182 mg (1.32 mmol) K_2CO_3 were used. The yield was 88% (198 mg).

General procedure for the photooxidation of thioanisole derivatives in the continuous flow system

10 mg of conjugated polyHIPE was packed into a transparent glass column (Omnifit, r = 0.35 cm, L = 7 cm) end-capped with two frits, equipped with PTFE-tubing. At a flowrate of 1 mL min^{-1}, 250 mg (2 mmol) of thioanisole (or other derivatives) in 20 mL solvent was pumped through the column continuously for a predetermined time period using a POSTNOVA PN 1610

pump. The column was irradiated with blue light LED lamp (4.5 W cm^2) at 460 nm (OSA Opto Lights). Samples were taken and conversion was determined by ^{1}H NMR.

Characterization

UV-vis absorption and emission spectra were recorded at room temperature on a Perkin Elmer Lambda 100 spectrophotometer and J&M TIDAS spectrofluorometer, respectively. Thermogravimetric analysis (TGA) was performed on a Mettler Toledo TGA-851 system. NMR measurements were recorded on Bruker AVANCE 250, Bruker AVANCE 500 or Bruker AVANCE 700 system. FT-IR sepctra were recorded on a Varian 1000 FT-IR spectrometer. Solid State NMR measurements were carried out using Bruker Avance II solid state NMR spectrometer operating at 300 MHz Larmor frequency equipped with a standard 4mm magic angle spinning (MAS) double resonance probe head. Scanning electron microscope (SEM) images were acquired on a LEO Gemini 1530 (Carl Zeiss AG, Germany) using an in lens SE detector. Transmission electron microscopy (TEM) images were acquired on a JEOL JEM-1400. Polymer surface areas and pore size distributions were measured by nitrogen adsorption and desorption at 77.3 K using Quadrasorb SI (Quantachrome Instruments). Data was evaluated using QuadraWin software from Quantachrome Instruments. Pore size distributions and pore volumes were derived from the adsorption branches of the isotherms using Quenched Solid Density Functional Theory (QSDFT, N_2, assuming carbon adsorbent with slit pores). Samples were degassed at 100 ^oC for 24 h under high vacuum before analysis.

2. Monomer Characterizations

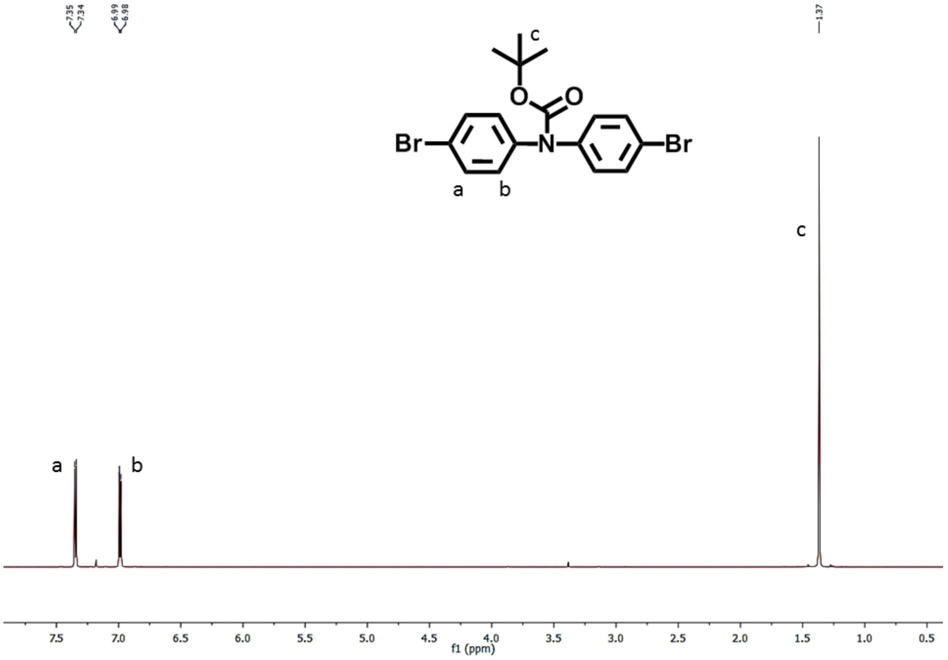

Figure S1. ^{1}H NMR spectrum of Boc-NPh$_2$.

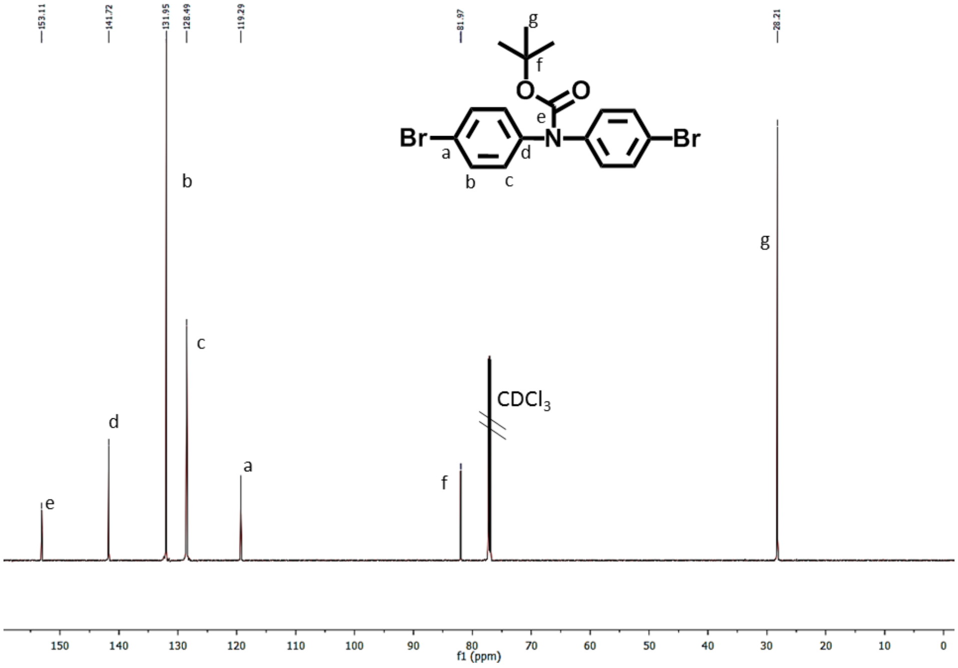

Figure S2. ^{13}C NMR spectrum of Boc-NPh$_2$.

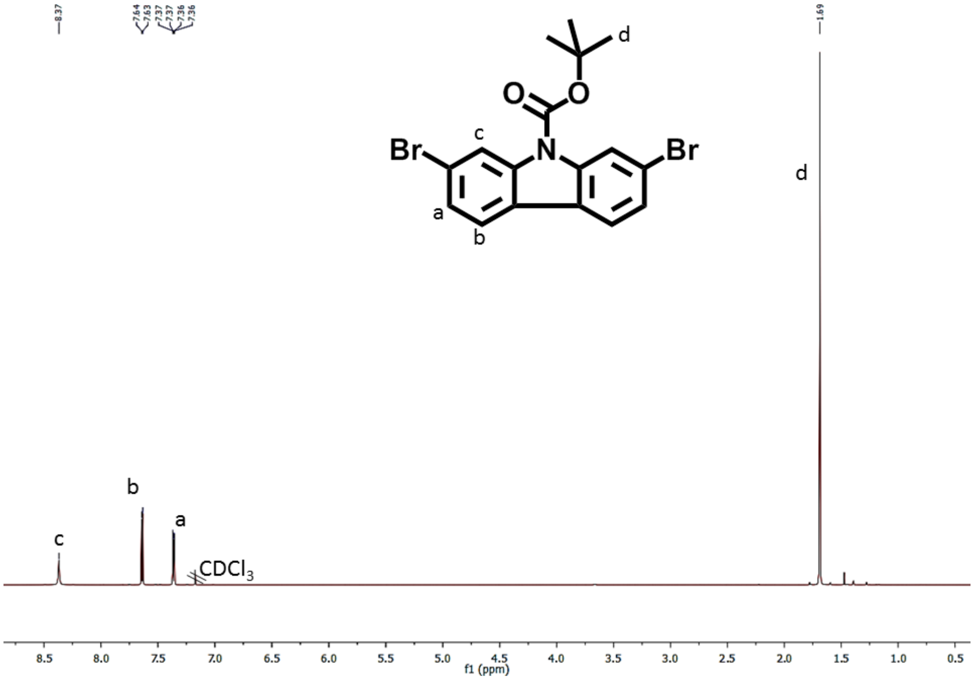

Figure S3. ^{1}H NMR spectrum of Boc-CB.

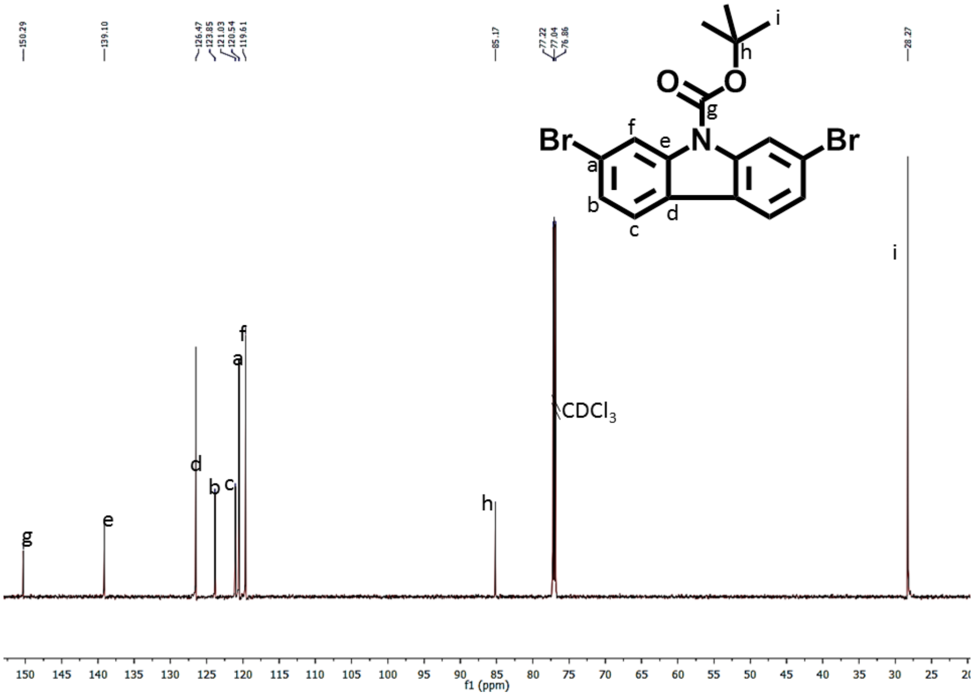

Figure S4. ^{13}C NMR spectrum of Boc-CB.

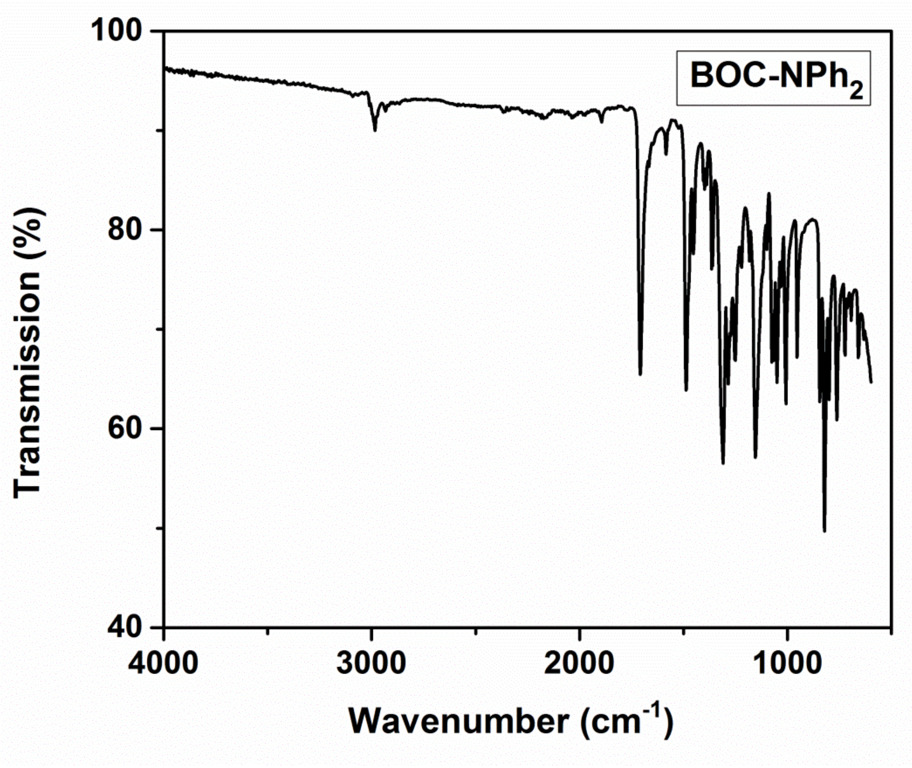

Figure S5. FTIR spectrum of Boc-NPh$_2$.

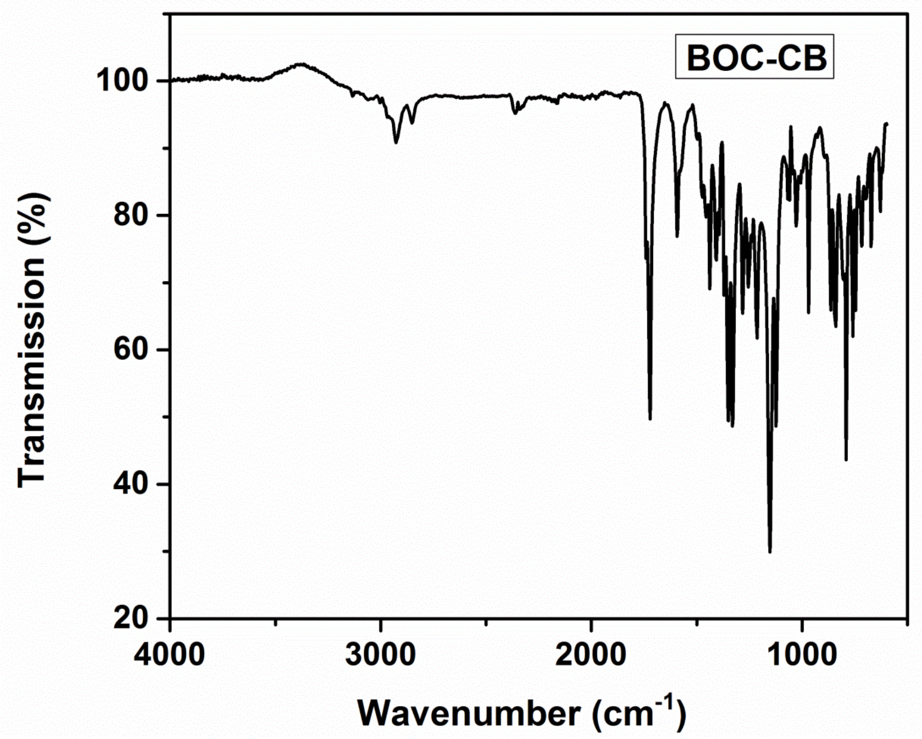

Figure S6. FTIR spectrum of Boc-CB.

3. FT IR Spectroscopy

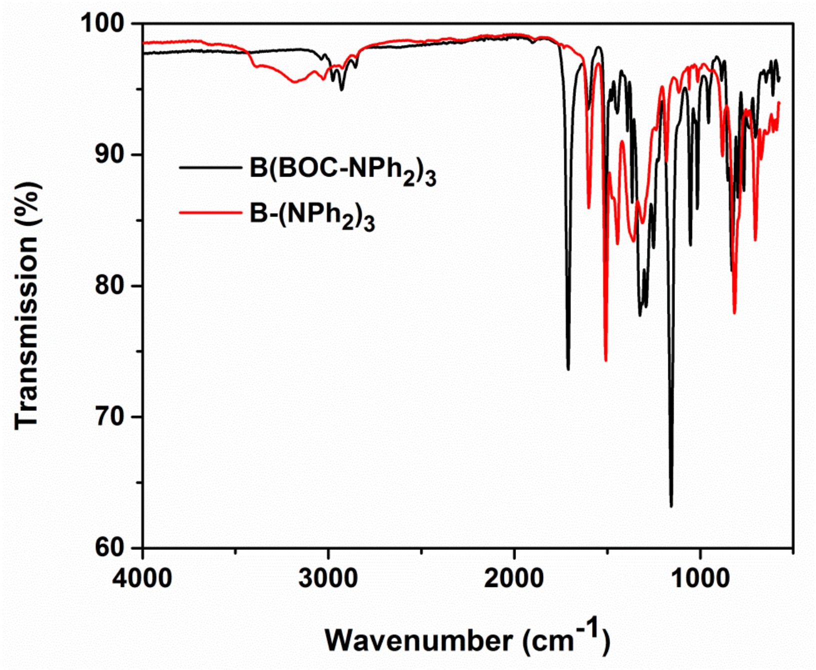

Figure S7. FTIR spectra of B-(Boc-NPh$_2$)$_3$ and B-(NPh$_2$)$_3$.

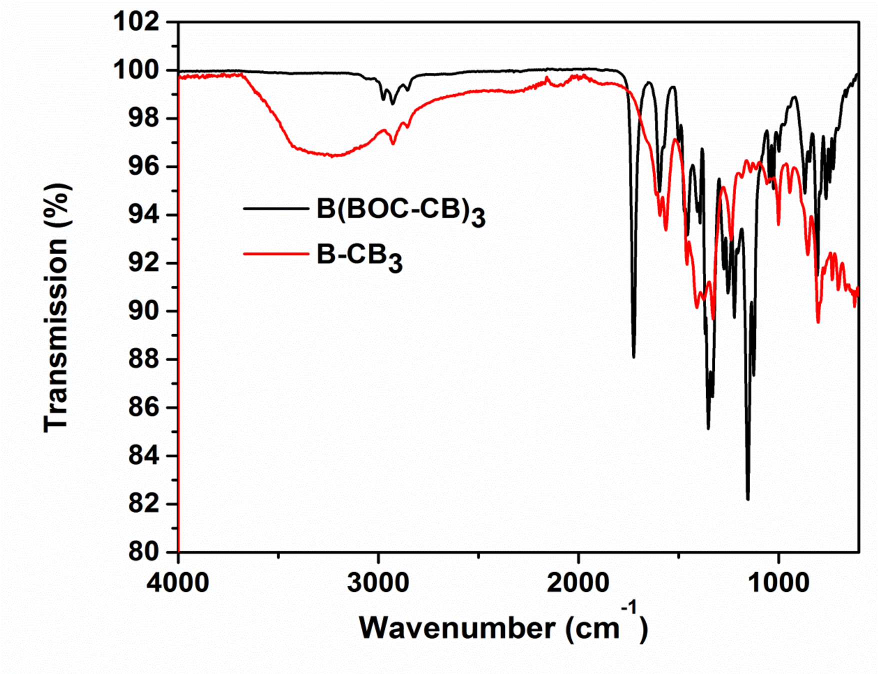

Figure S8. FTIR spectra of B-(Boc-CB)$_3$ and B-CB$_3$.

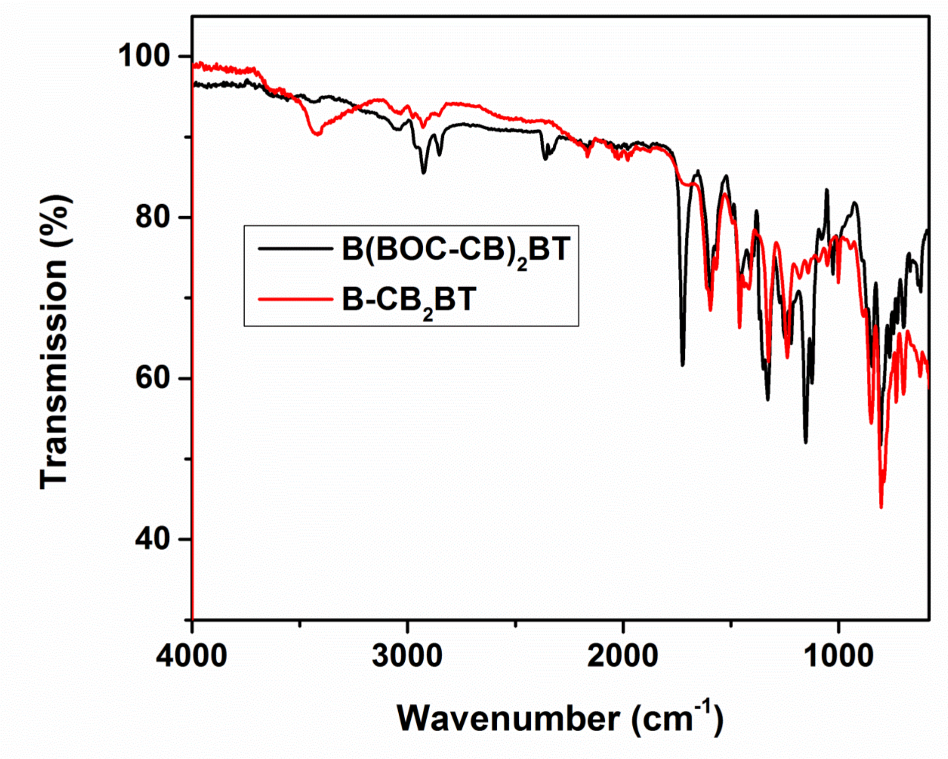

Figure S9. FTIR spectra of B-(BOC-CB)$_2$-BT and B-CB$_2$BT.

4. Fluorescence Spectroscopy

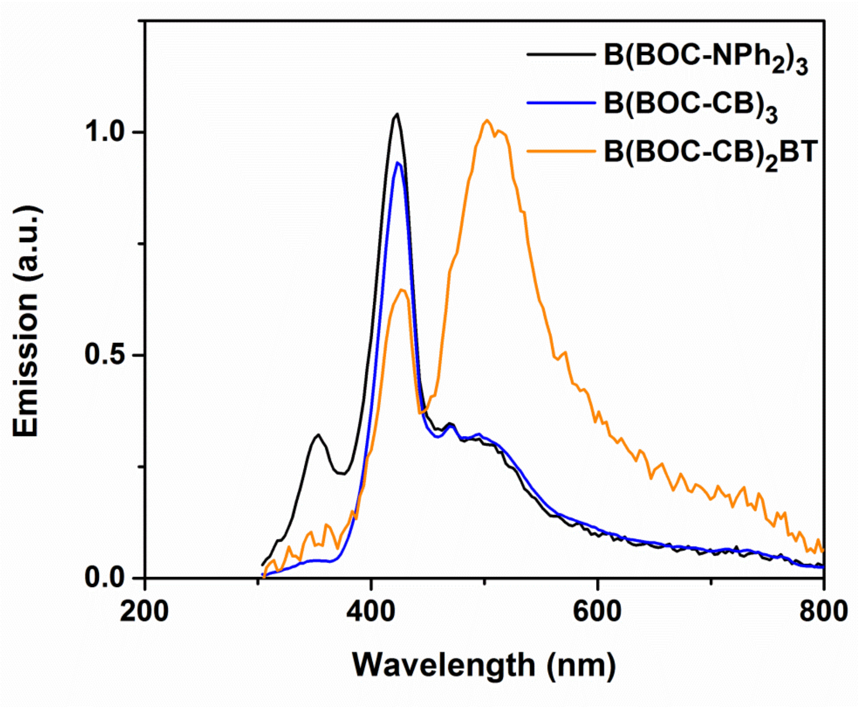

Figure S10. Fluorescence spectra of poly(HIPE)s with Boc groups.

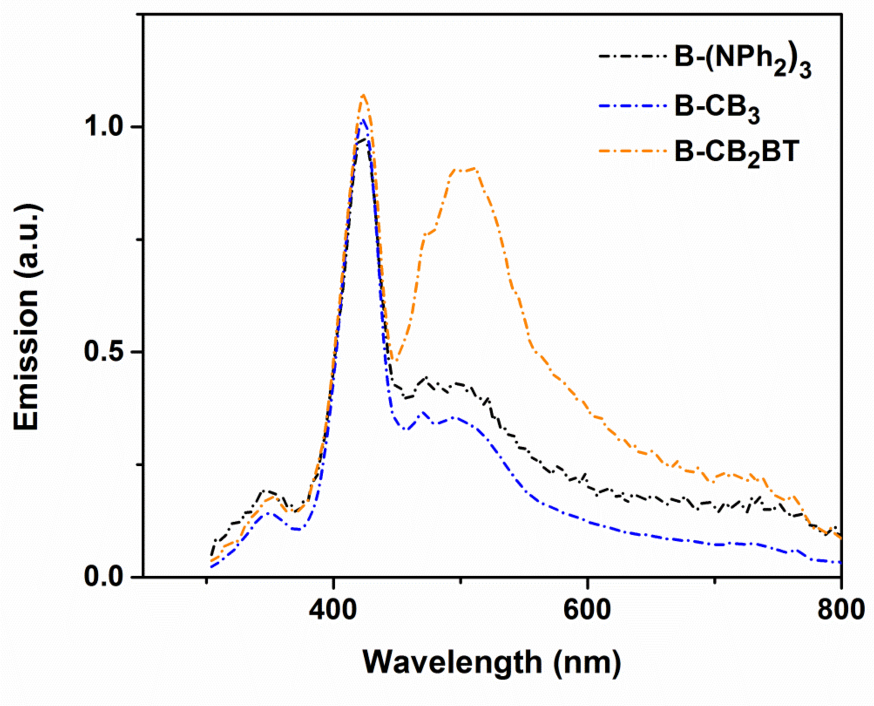

Figure S11. Fluorescence spectra of poly(HIPE)s without Boc groups.

5. Thermogravimetric Analysis (TGA)

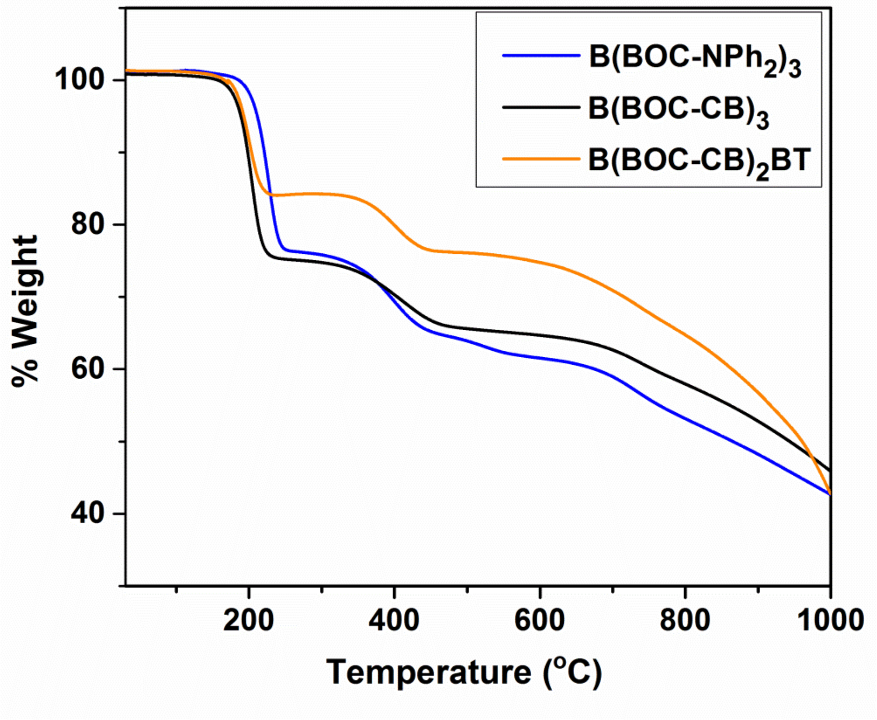

Figure S12. Thermogravimetric analysis of poly(HIPE)s with Boc groups.

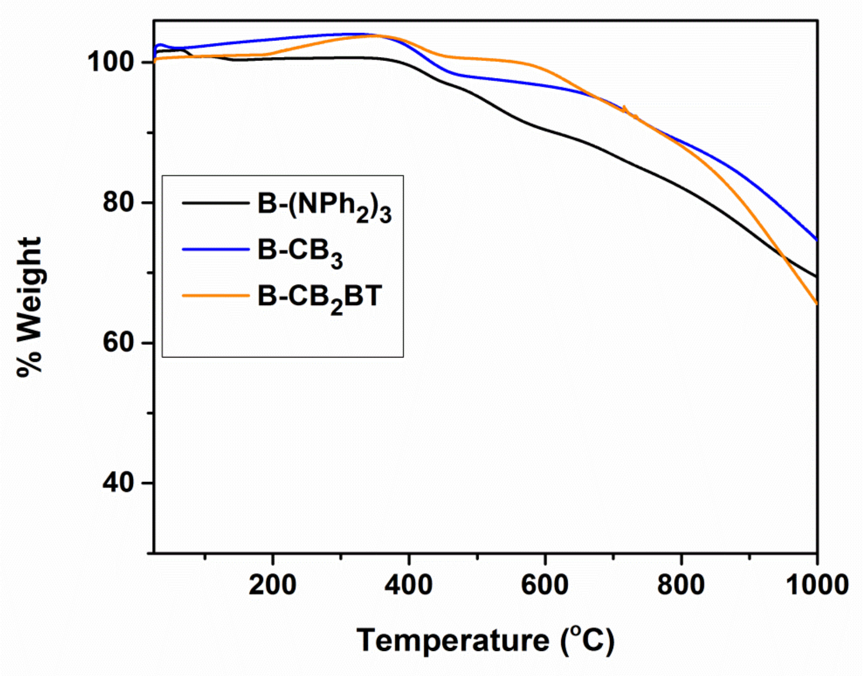

Figure S13. Thermogravimetric analysis of poly(HIPE)s without Boc groups.

6. Solid State ^{13}C CP/MAS NMR Spectroscopy

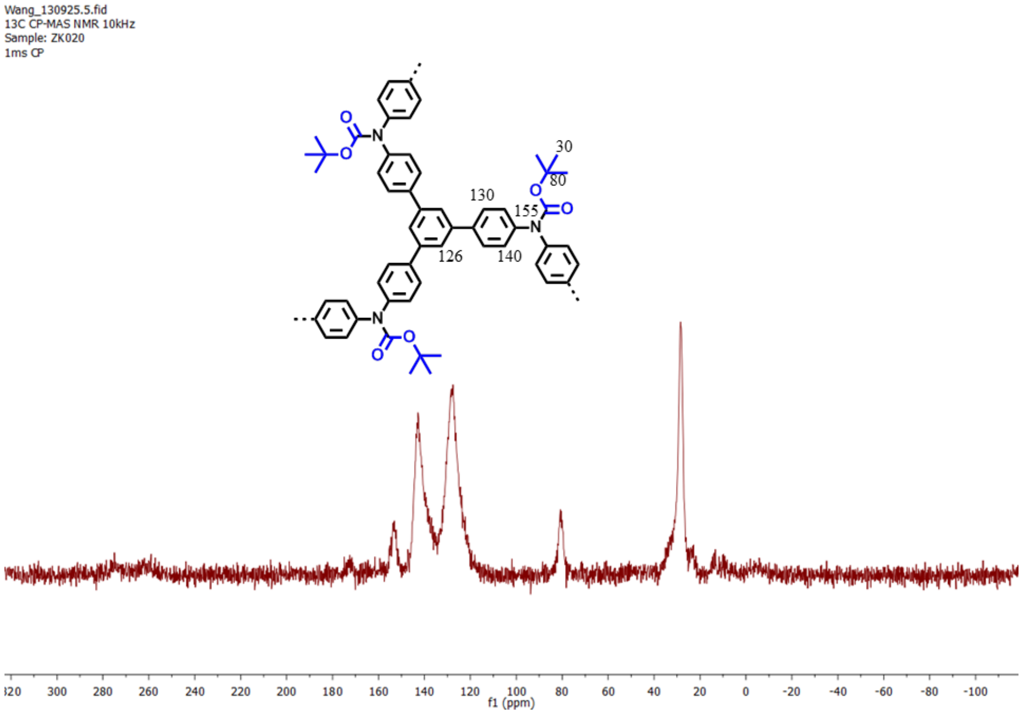

Figure S14. Solid state ^{13}C CP/MAS NMR spectrum of B(BOC-NPh$_2$)$_3$.

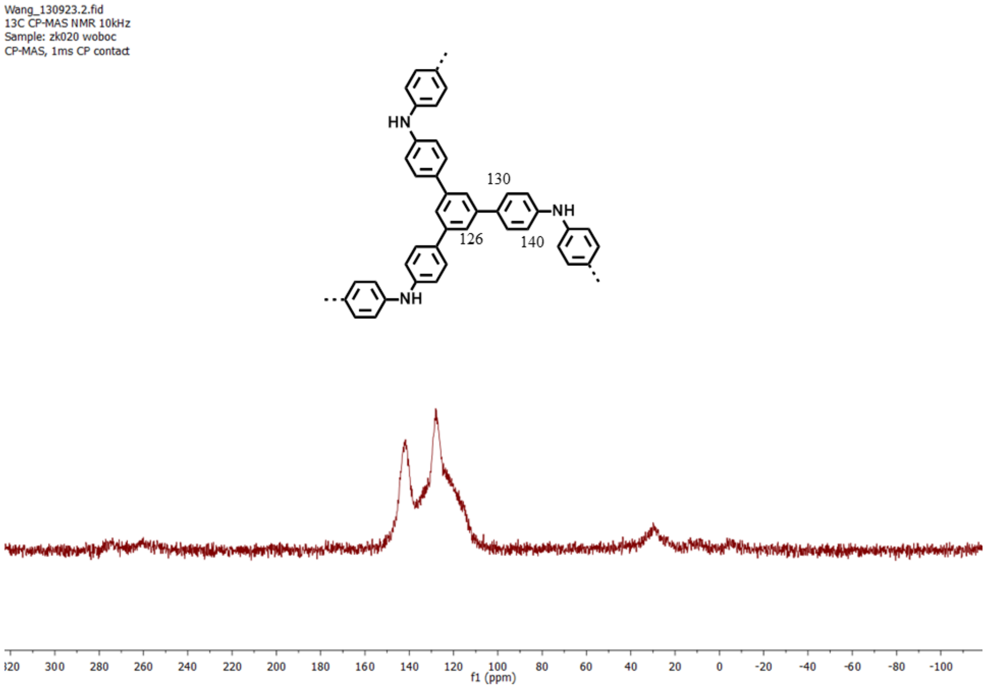

Figure S15. Solid state ^{13}C CP/MAS NMR spectrum of B-(NPh$_2$)$_3$.

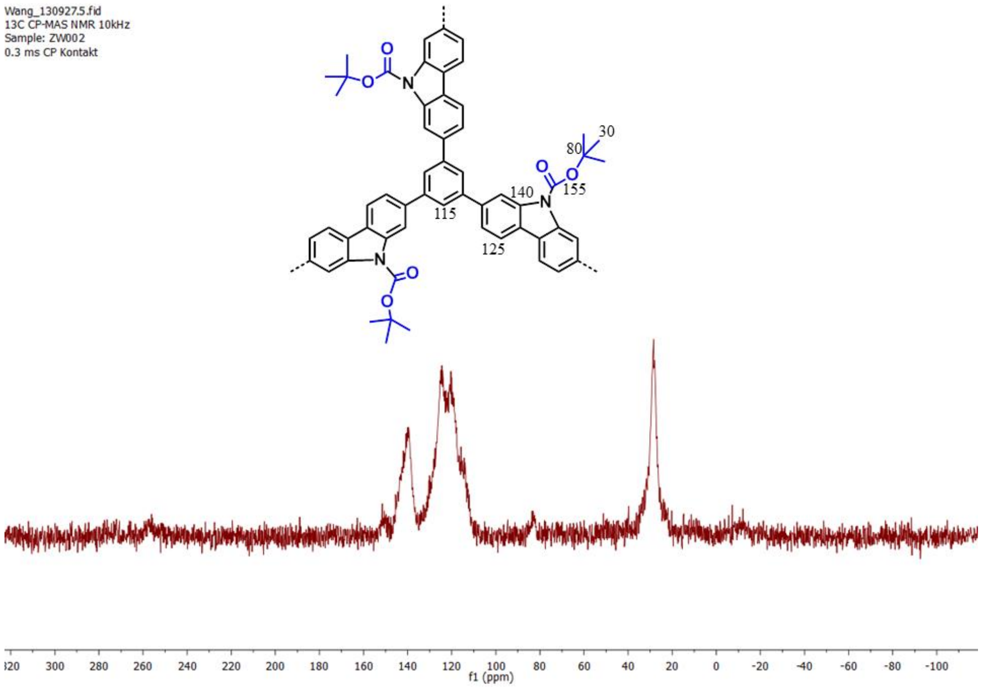

Figure S16. Solid state ^{13}C CP/MAS NMR spectrum of B(BOC-CB)$_3$.

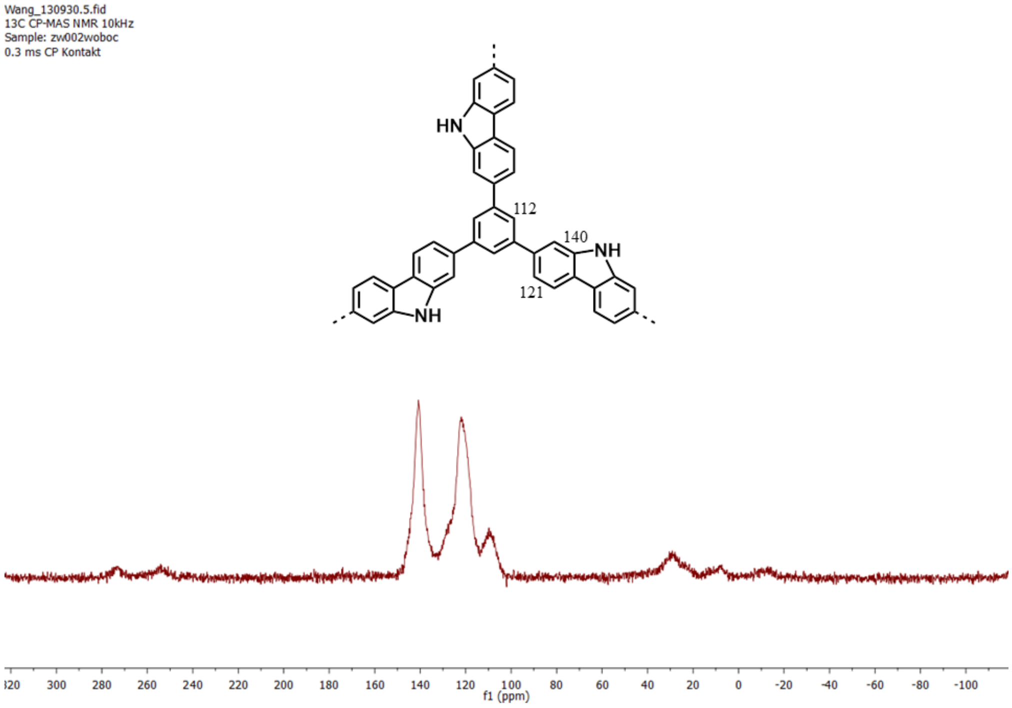

Figure S17. Solid state ^{13}C CP/MAS NMR spectrum of B-CB$_3$.

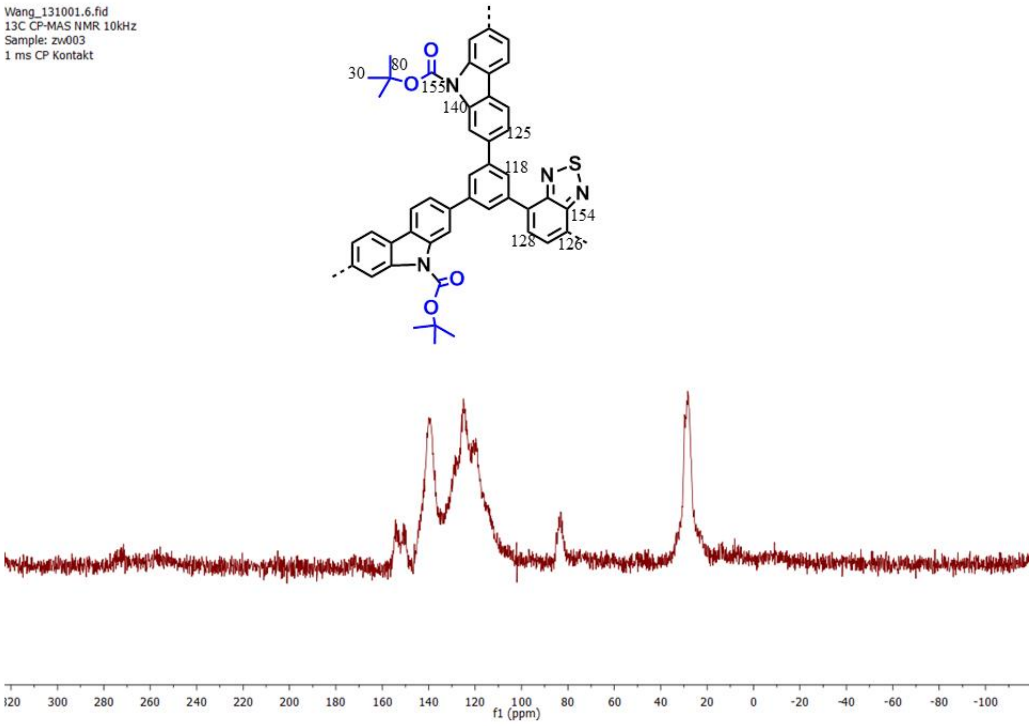

Figure S18. Solid state ^{13}C CP/MAS NMR spectrum of B-(BOC-CB)$_2$-BT.

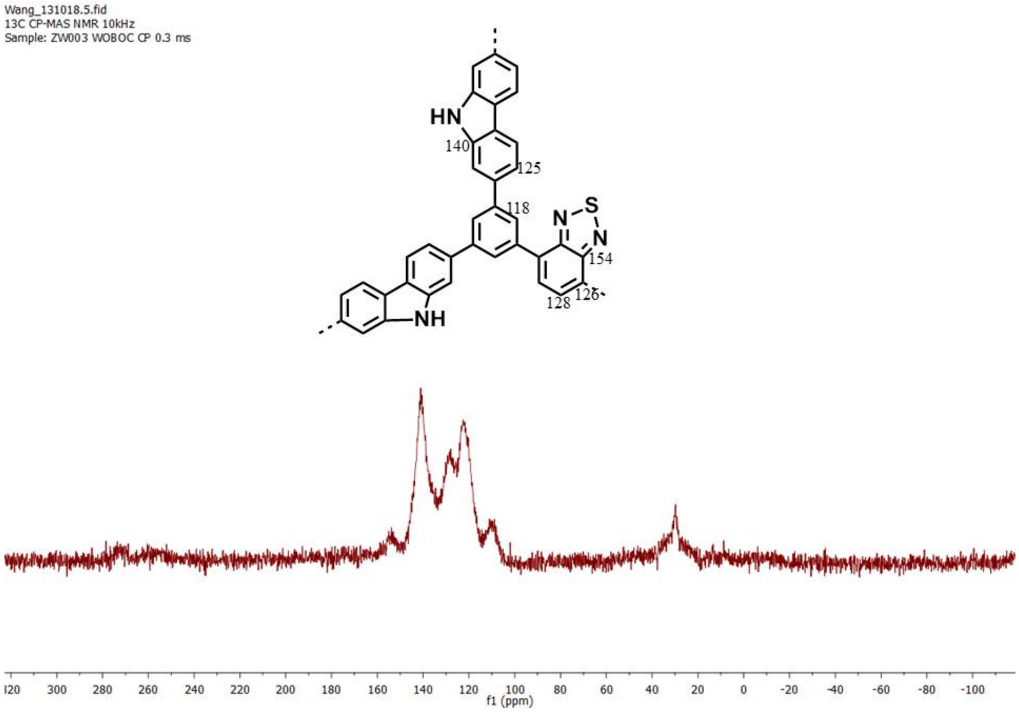

Figure 19. Solid state ^{13}C CP/MAS NMR spectrum of B-CB$_2$-BT.

7. Brunauer-Emmett-Teller (BET) Surface Area and Pore Size Measurements

Table S1. Surface area and pore size characterizations of various poly(HIPE)s.

PolyHIPE	Surface Area (m^2/g)	Pore Diameter (nm)	Pore Volume (cm^3/g)
B-(Boc-NPh$_2$)$_3$	45	1.5	0.066
B-(Boc-CB)$_3$	27	2.7	0.051
B-(Boc-CB)$_2$-BT	26	2.9	0.056
B-(NPh$_2$)$_3$	198	1.5	0.161
B-CB$_3$	229	1.5	0.169
B-CB$_2$-BT	53	1.5	0.065

8. N_2 Sorption Isotherms and Pore Size and Distribution

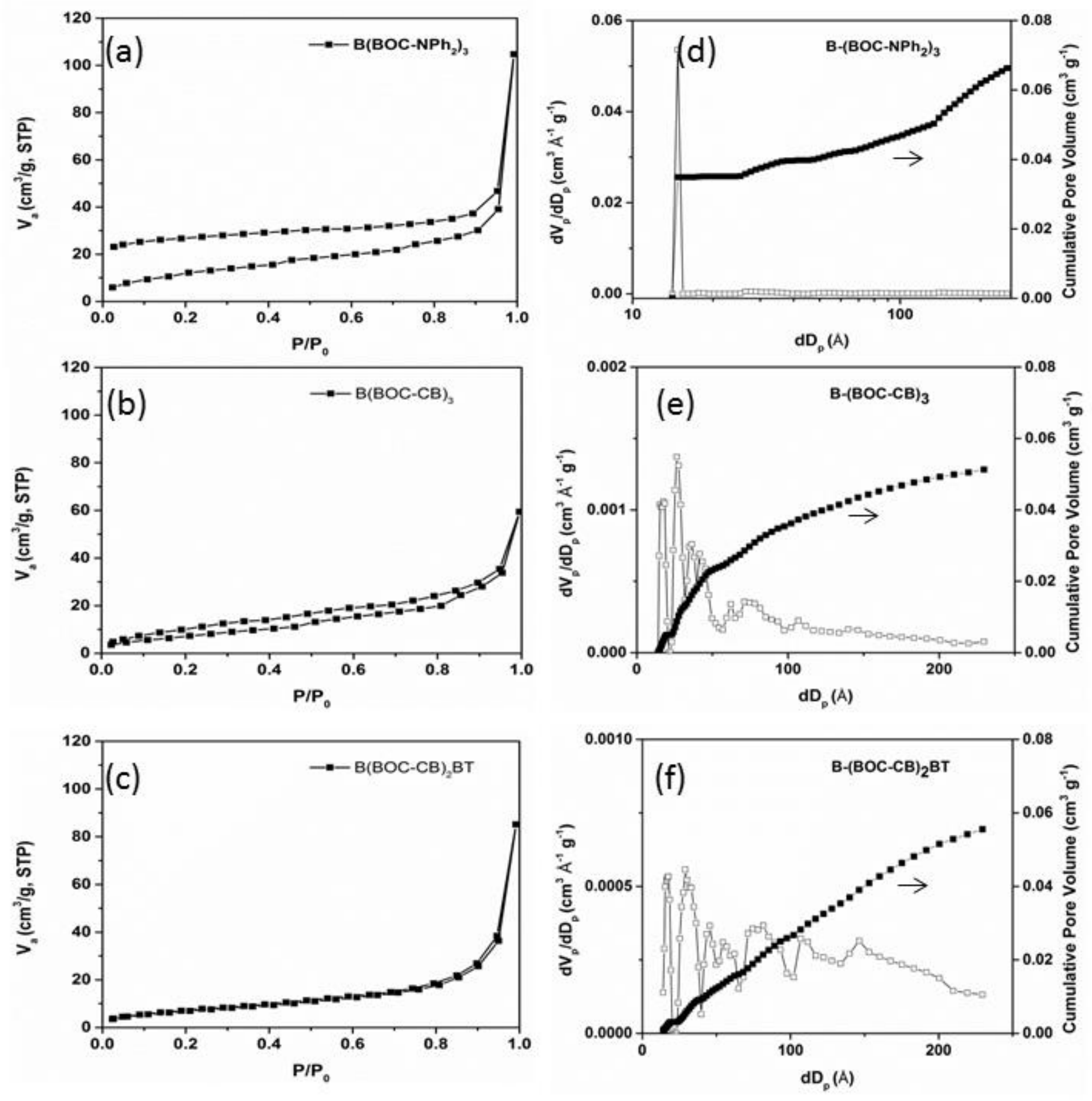

Figure S20. N_2 Sorption Isotherms and Pore Size Distributions of poly(HIPE)s with Boc groups.

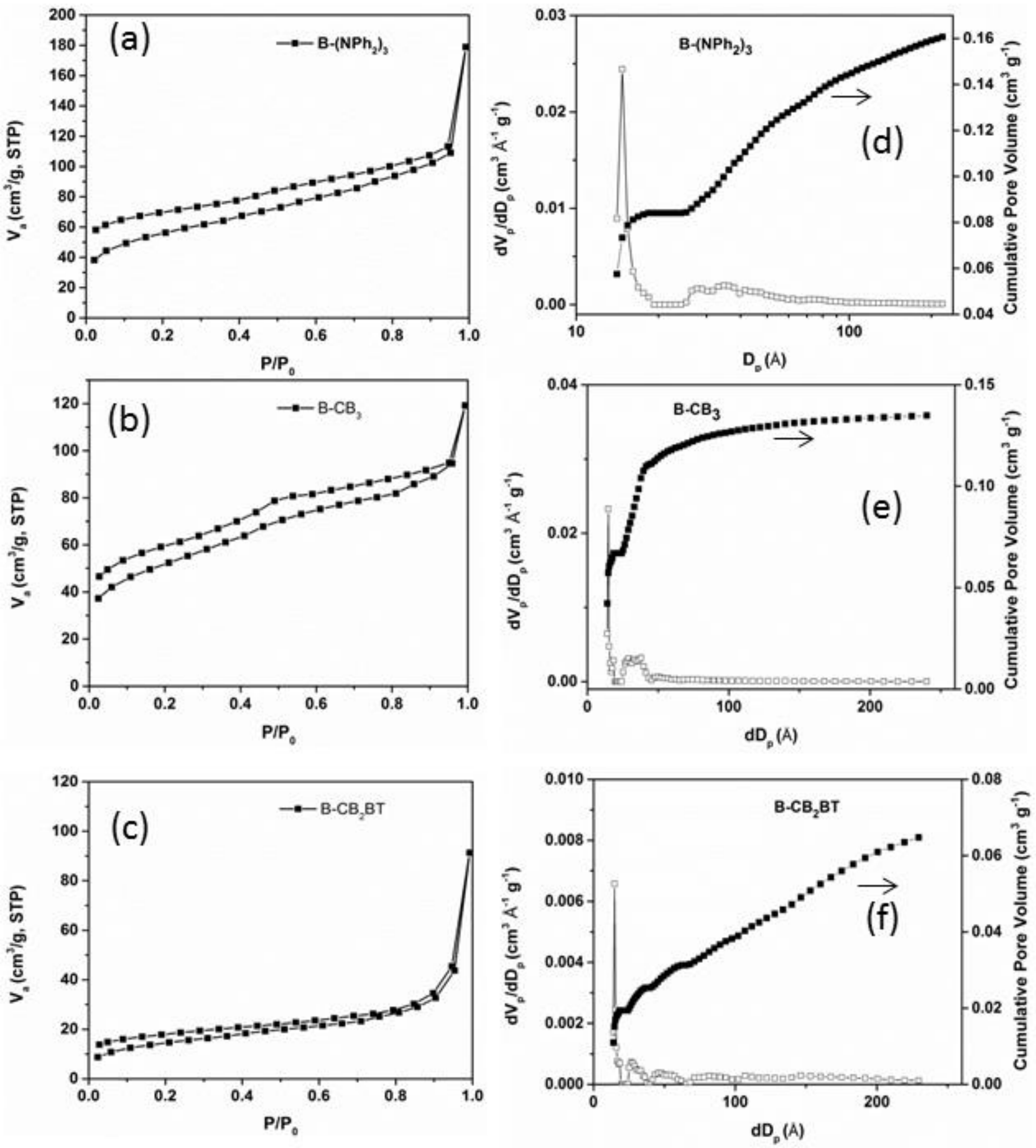

Figure S21. N_2 Sorption Isotherms and Pore Size Distributions of poly(HIPE)s without Boc groups.

9. ^{1}H NMR Spectra and Repeating Experiments for Photooxidation of Thioanisole

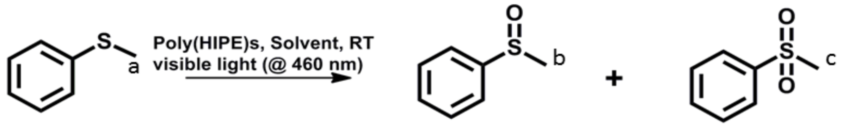

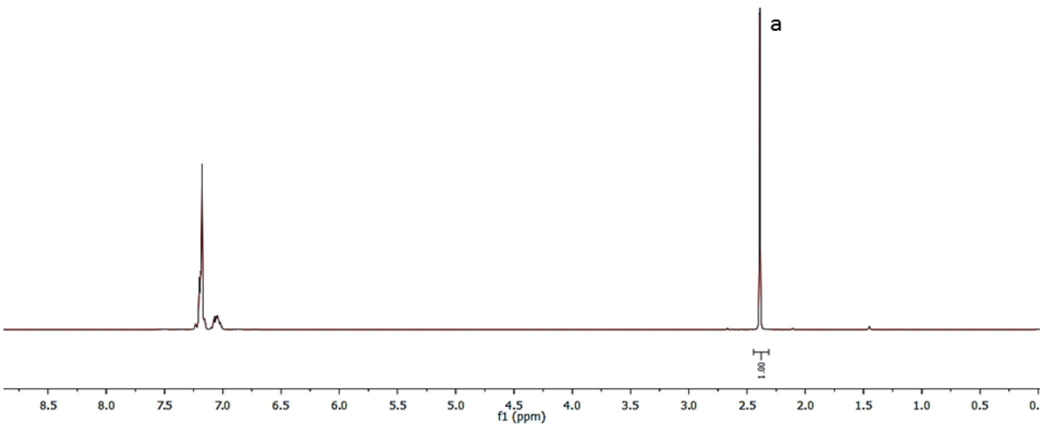

Figure S22. ^{1}H NMR spectrum of thioanisole before photooxidation reaction.

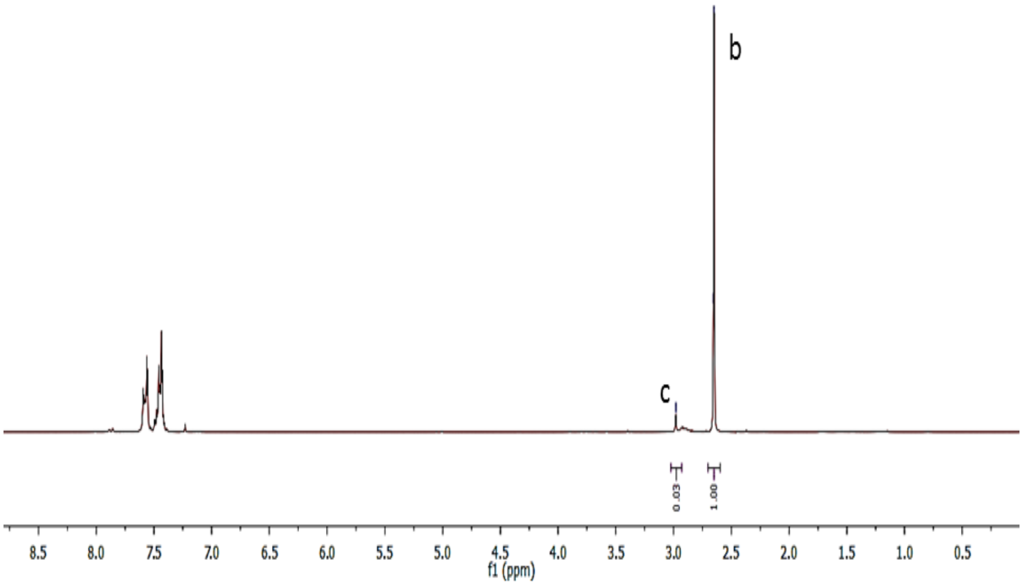

Figure S23. ^{1}H NMR spectrum of products after photooxidation reaction.

Table S2. Repeating experiments of the selective photooxidation of thiolanisole.

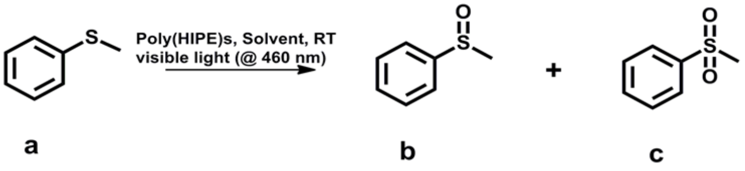

Entry	Time (h)	Conversion (%)	Selectivity (%)	
			b	c
1	24	>99	95	5
2	24	>99	94	6
3	24	>99	97	3
4	24	>99	99	1
5	24	97	>99	<1
6	24	98	>99	<1

10. Density function theory (DFT) calculations

Table S3: HOMO-LUMO levels of the polymers calculated with Gaussian 09 using the density function theory RB3LYP/6311G method.

Polymer	HOMO / eV		LUMO / eV		Band gap / eV	
	Star-shaped repeating unit	**Ring structure**	**Star-shaped repeating unit**	**Ring structure**	**Star-shaped repeating unit**	**Ring structure**
B-(Boc-NPh$_2$)$_3$	-5.94	-5.95	-1.28	-1.26	4.66	4.67
B-(NPh$_2$)$_3$	-5.22	-5.39	-0.96	-1.16	4.27	4.22
B-(Boc-CB)$_3$	-5.80	-5.65	-1.38	-1.65	4.43	4.00
B-CB$_3$	-5.74	-5.63	-1.28	-1.47	4.46	4.17
B-(Boc-CB)$_2$-BT	-5.83	-5,76	-2.89	-3.10	2.94	2.66
B-CB$_2$-BT	-5.74	-5.69	-2.99	-3.07	2.76	2.62

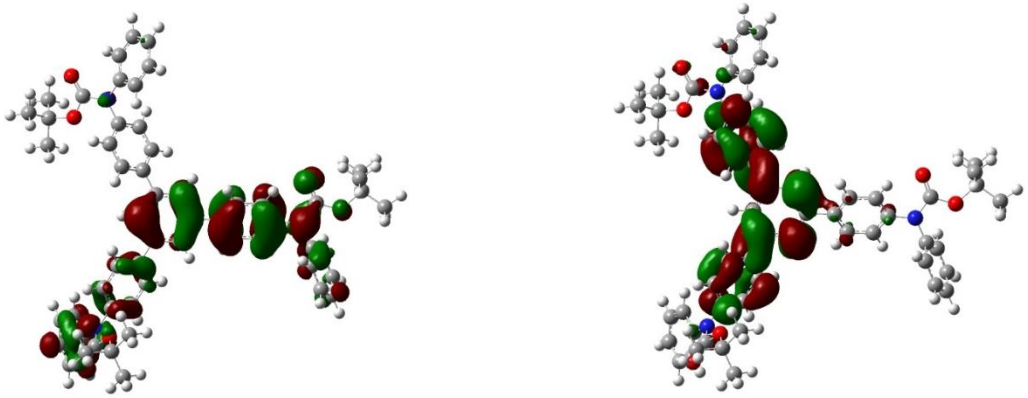

HOMO LUMO

B-(Boc-NPh$_2$)$_3$

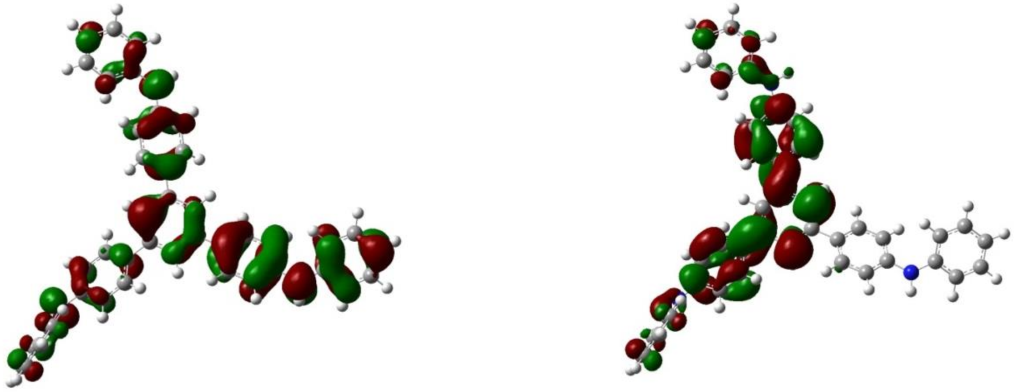

HOMO LUMO

B-(NPh$_2$)$_3$

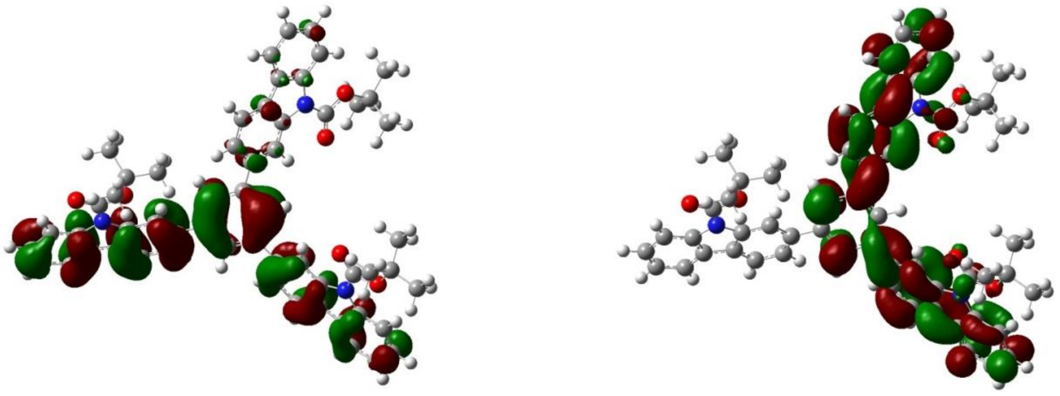

HOMO LUMO

B-(Boc-CB)$_3$

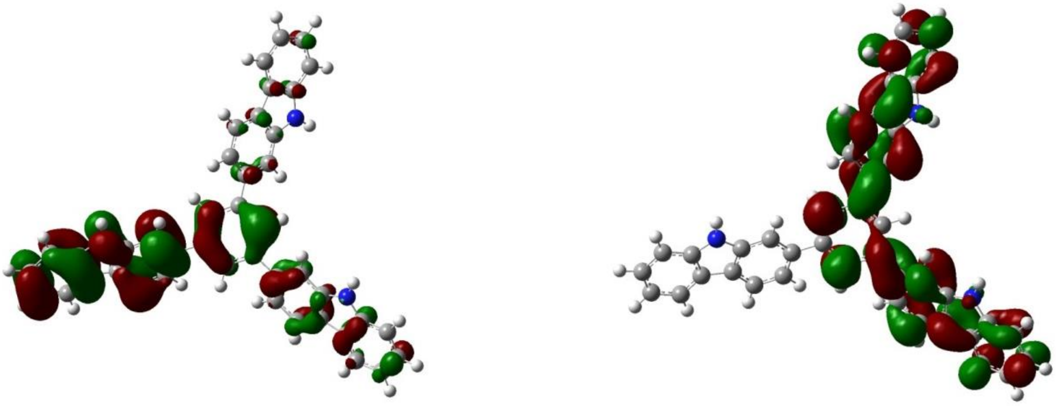

HOMO LUMO

B-CB$_3$

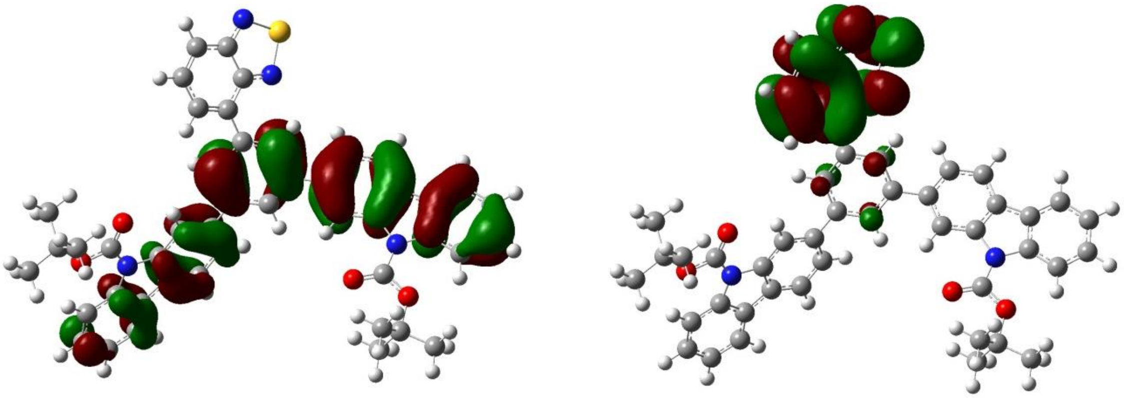

HOMO LUMO

B-(Boc-CB)$_2$-BT

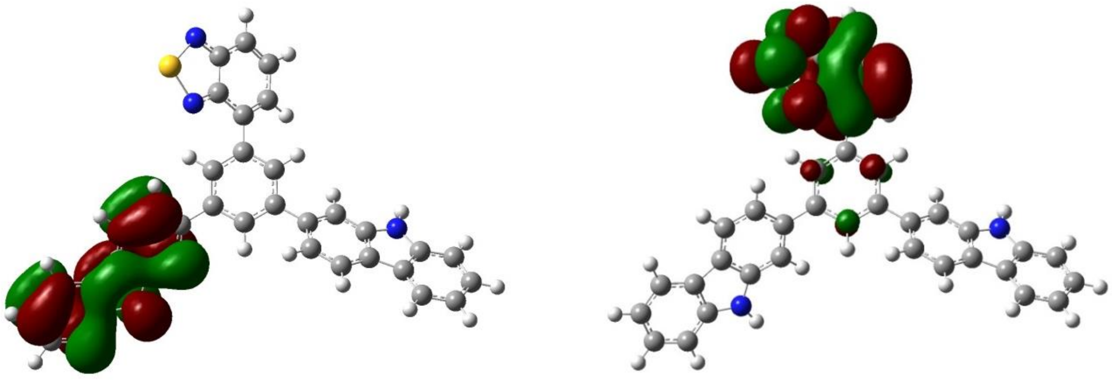

Homo LUMO

B-CB$_2$-BT

Figure S24. HOMO-LUMO band structures of the star-shaped repeating units.

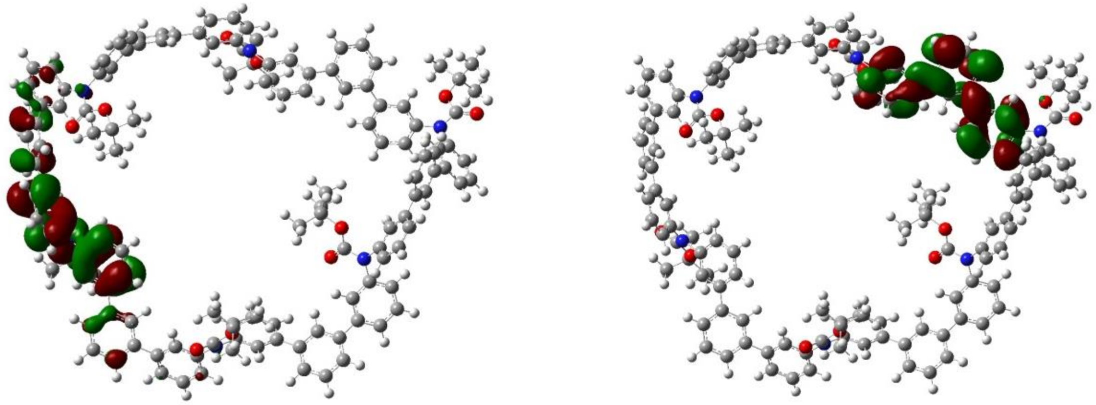

HOMO LUMO

B-(Boc-NPh$_2$)$_3$

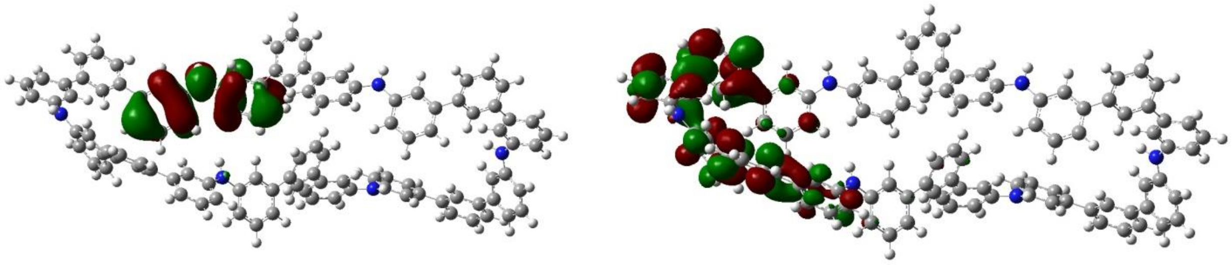

HOMO LUMO

B-(NPh$_2$)$_3$

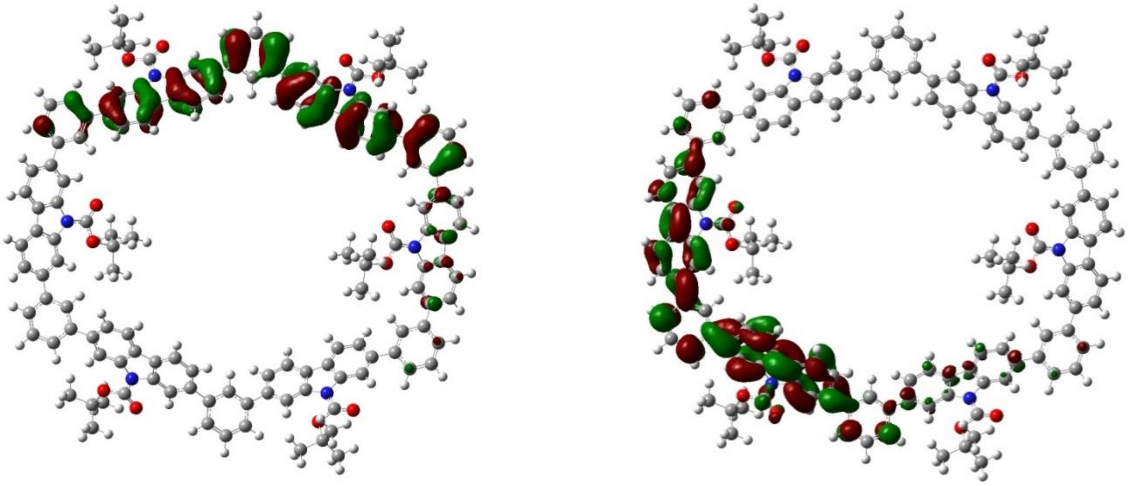

HOMO LUMO

B-(Boc-CB)$_3$

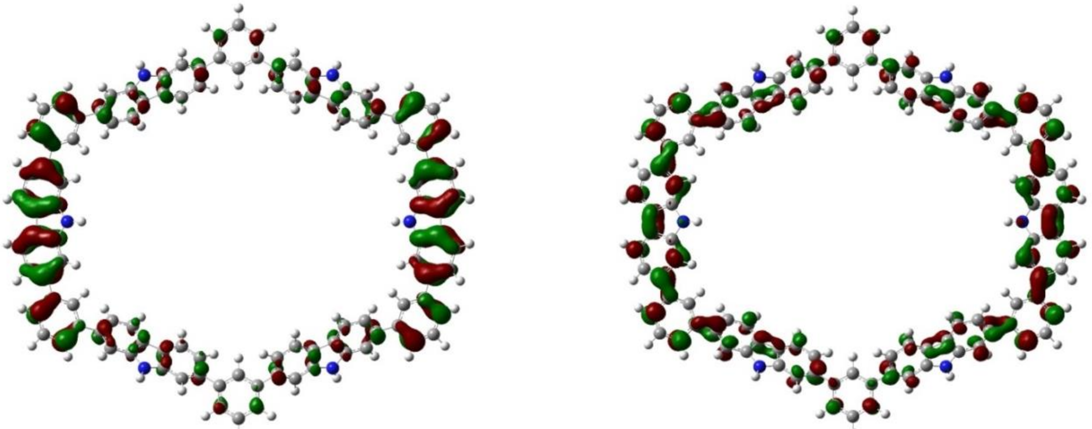

HOMO LUMO

B-CB$_3$

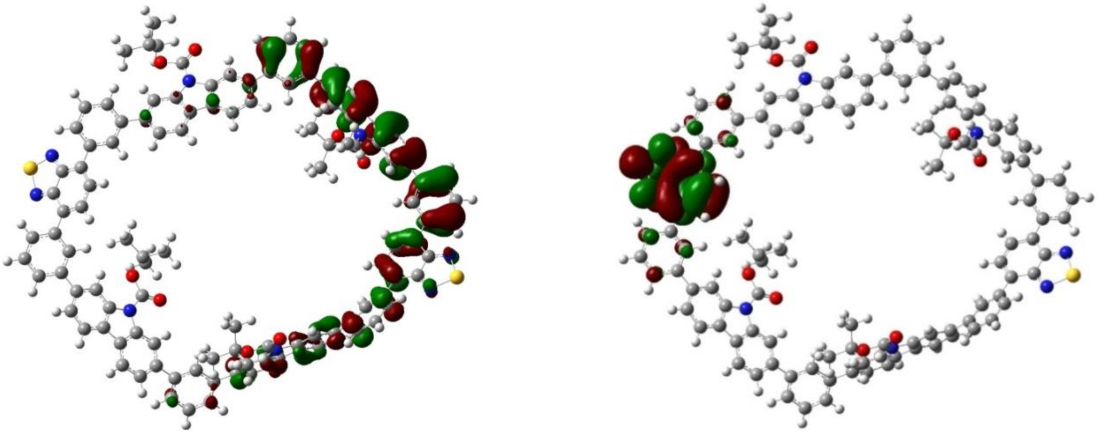

HOMO LUMO

B-(Boc-CB)$_2$-BT

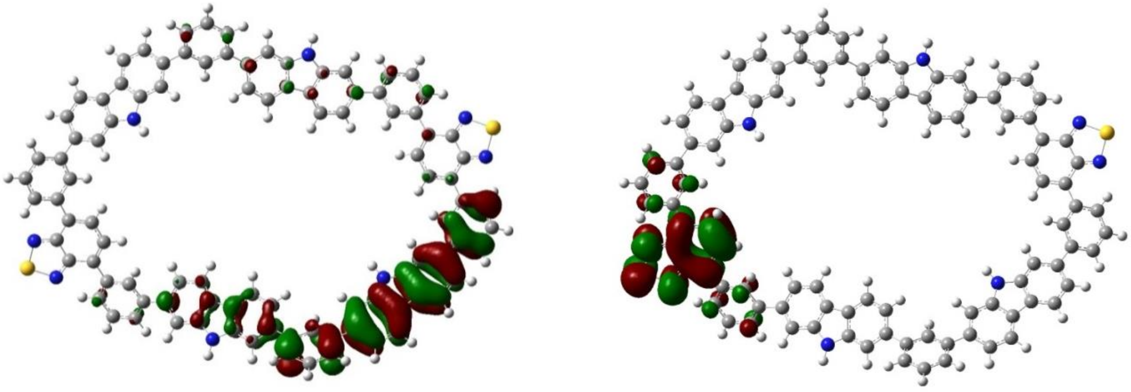

HOMO LUMO

B-CB$_2$-BT

Figure S25. HOMO-LUMO band structures of the idealized ring structures.

11. Additional SEM Images of PolyHIPEs

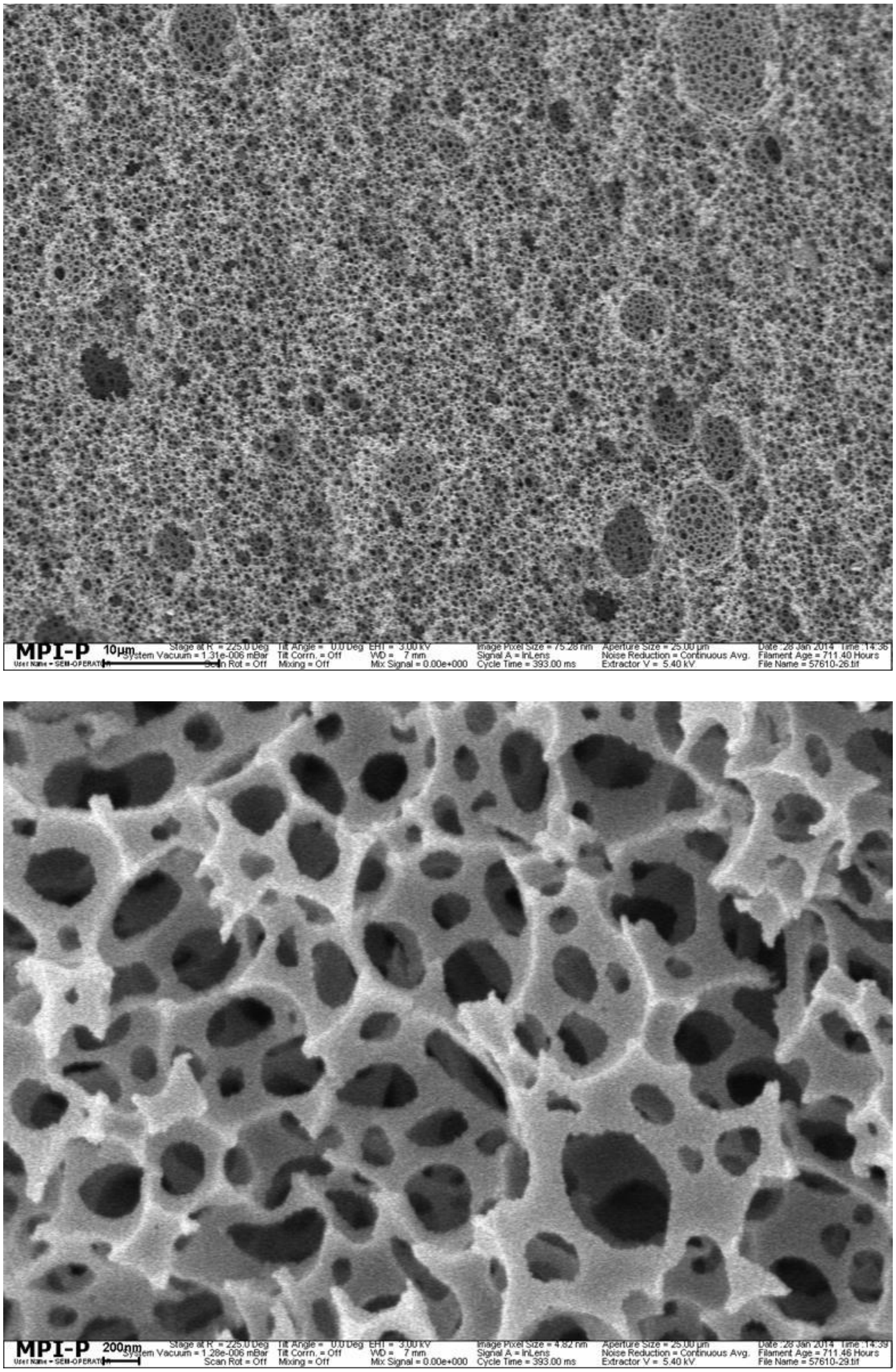

Figure S26. SEM image of B-(Boc-NPh_2)$_3$.

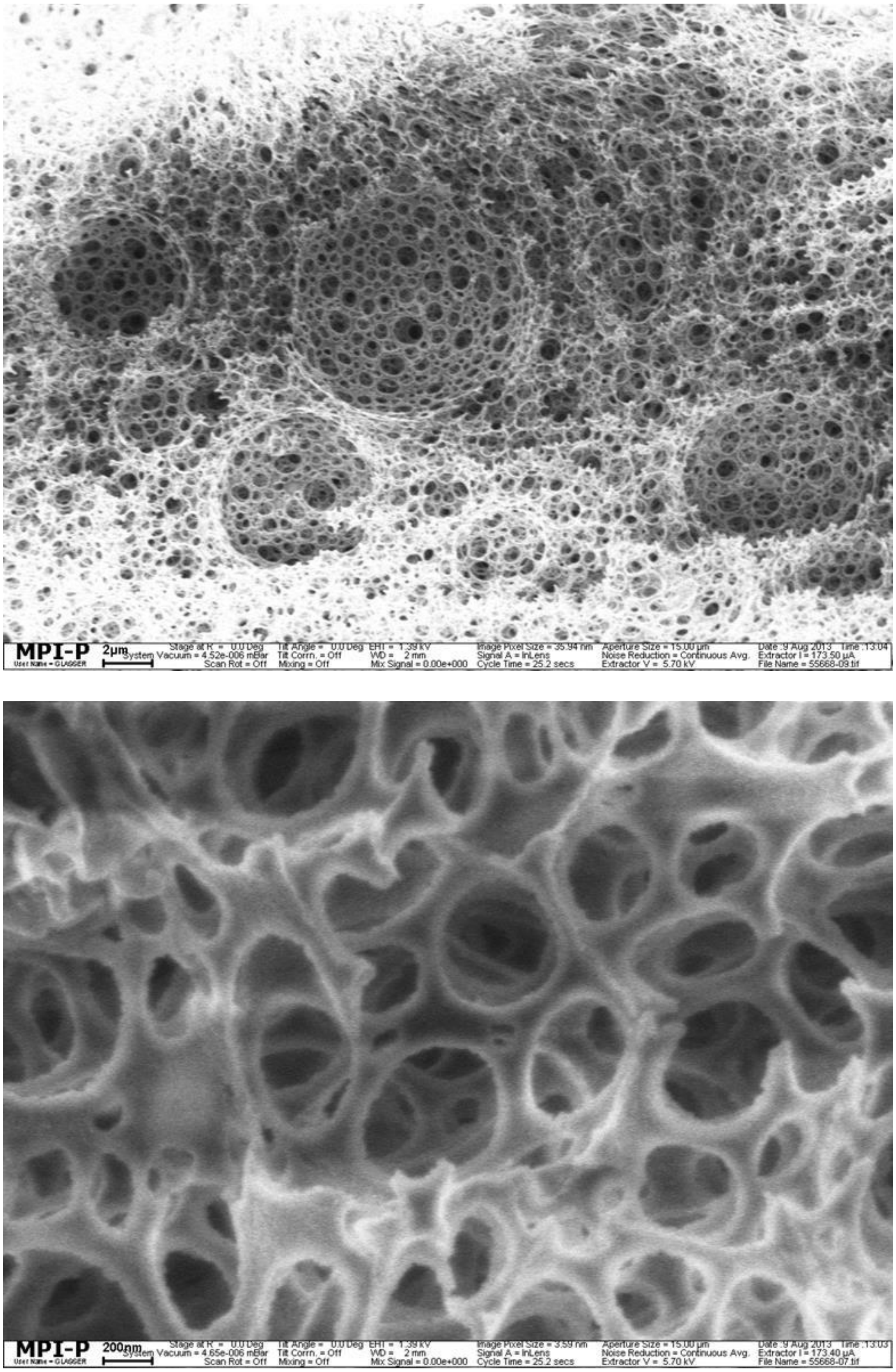

Figure S27. SEM image of B-$(NPh_2)_3$.

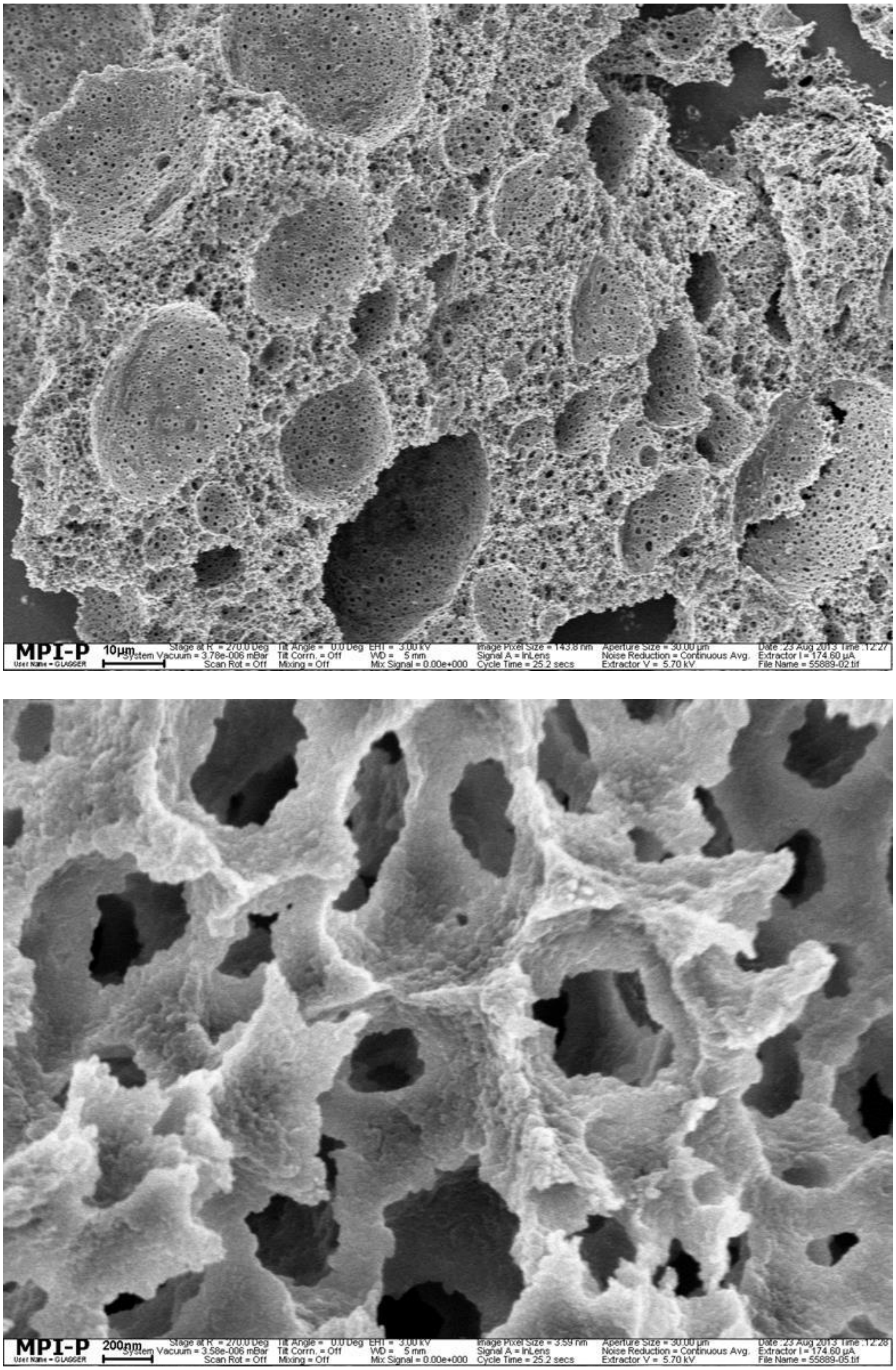

Figure S28. SEM image of B-(BOC-CB)$_3$.

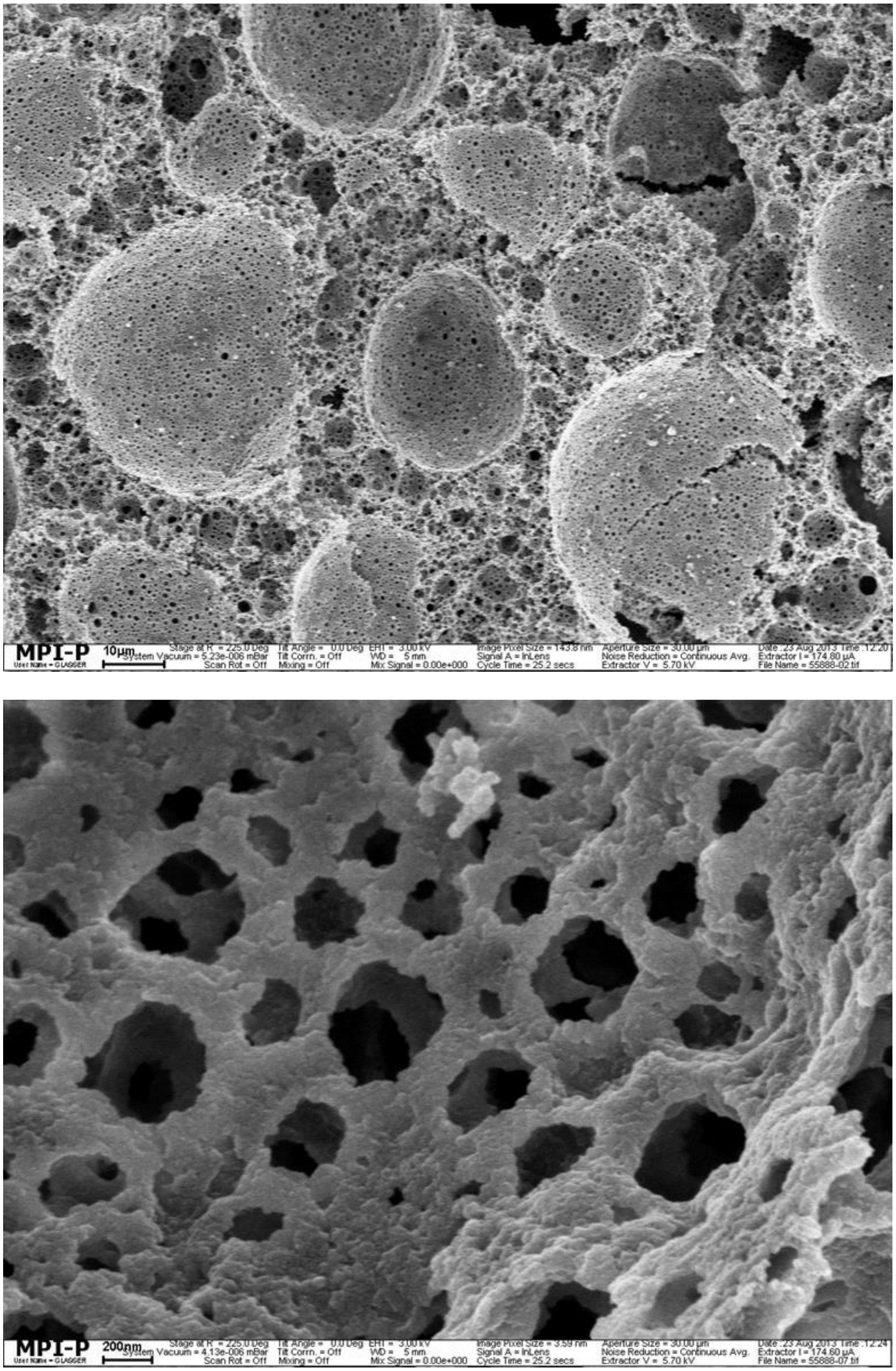

Figure S29. SEM image of B-CB_3.

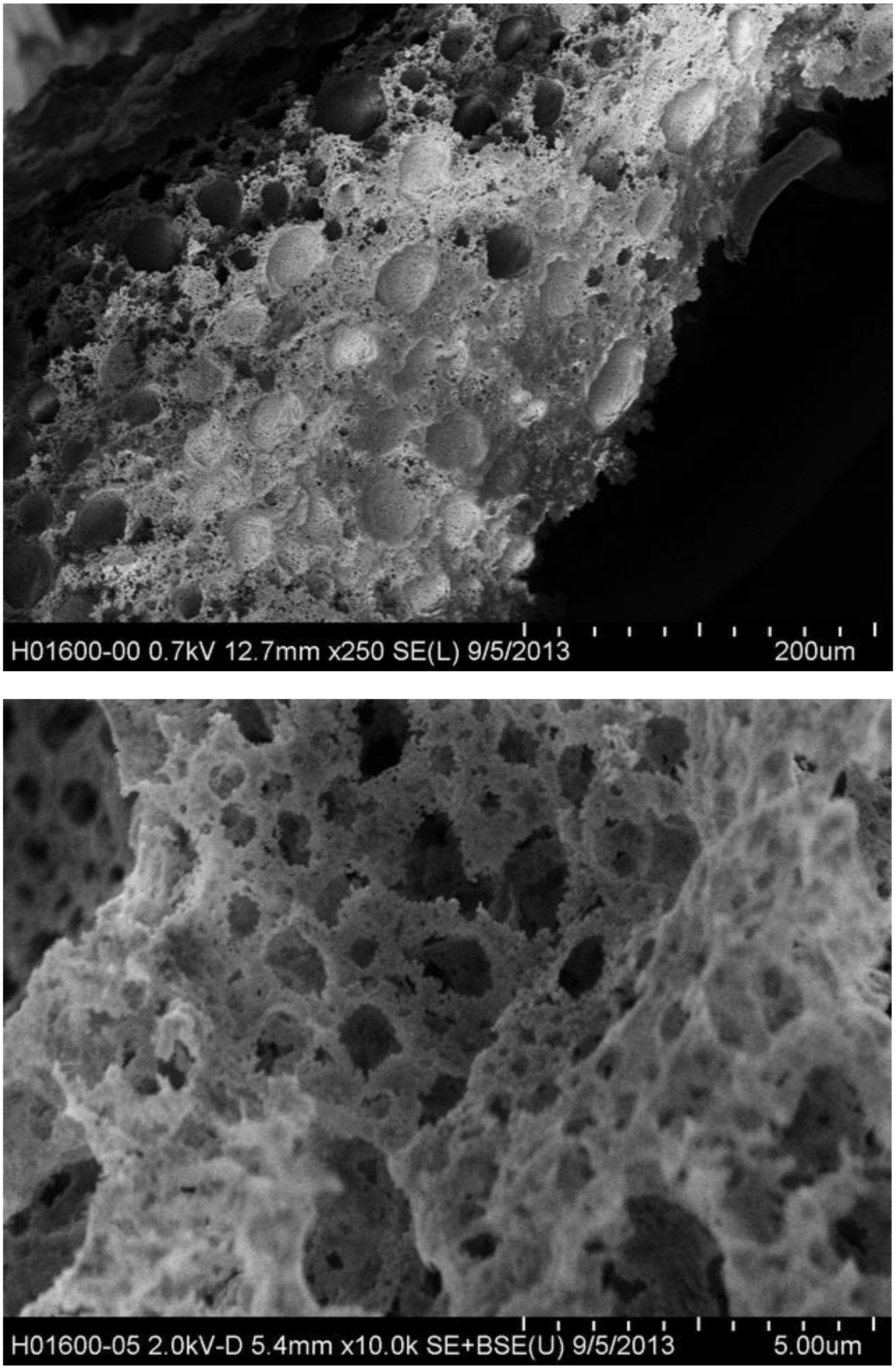

Figure S30. SEM image of B-$(BOC\text{-}CB)_2$-BT.

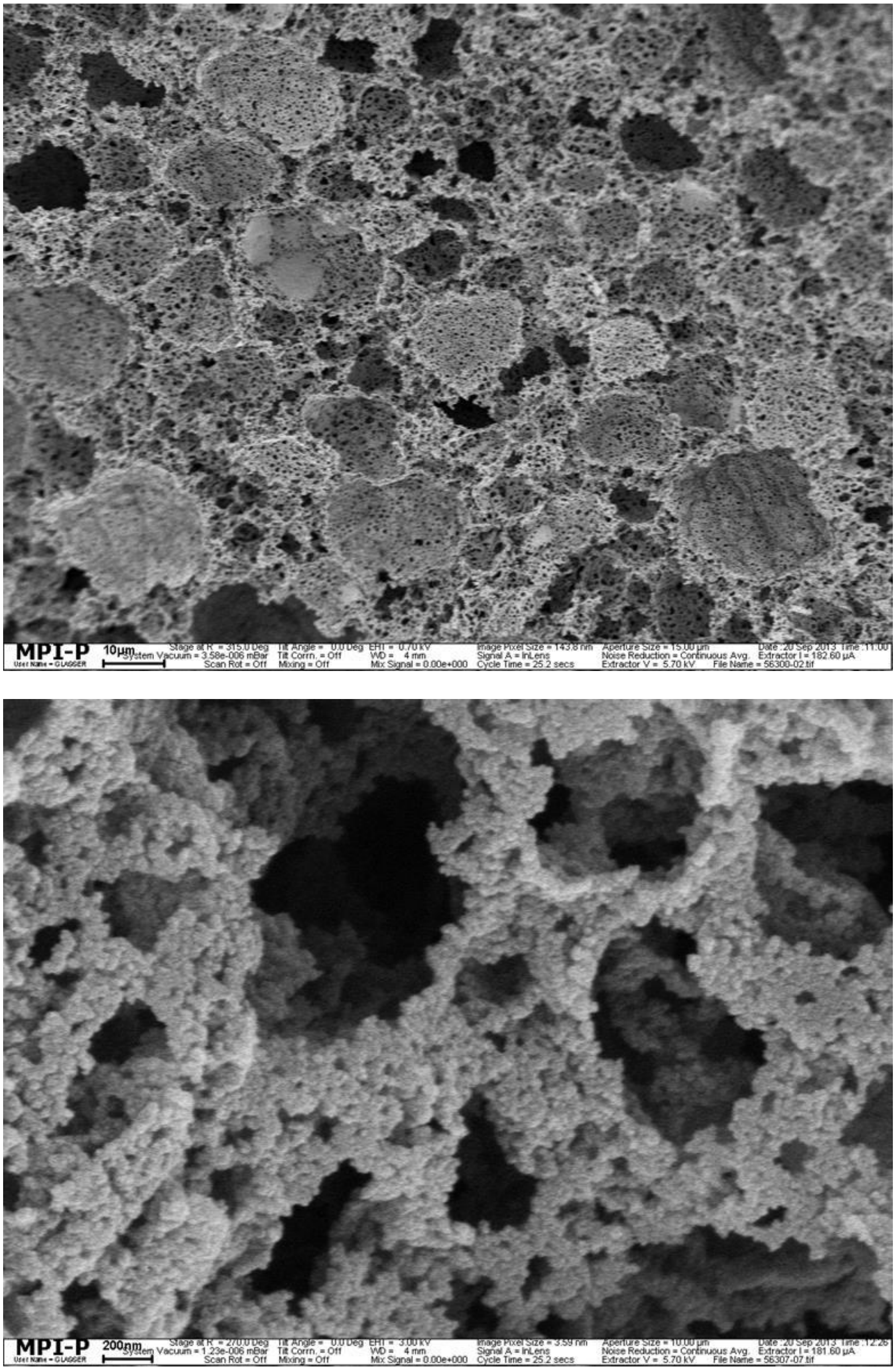

Figure S31. SEM image of B-CB_2-BT.

TEM Images of PolyHIPEs

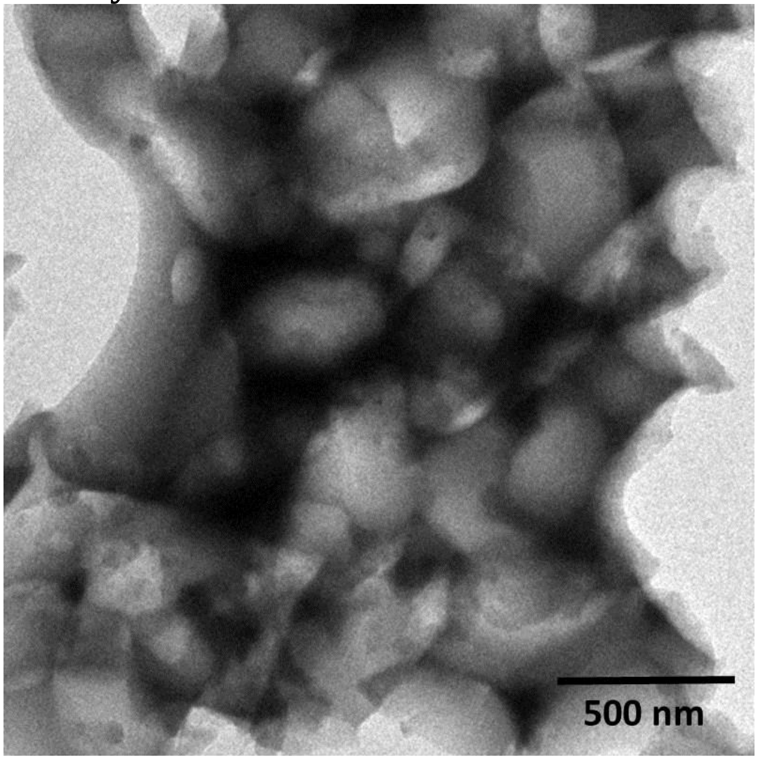

Figure S32. SEM image of B-(Boc-NPh_2)$_3$.

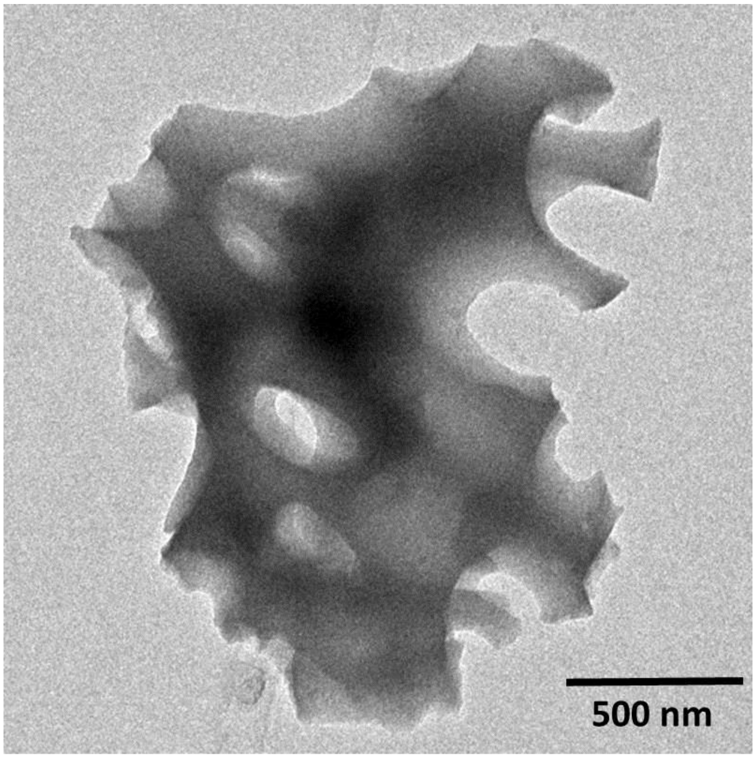

Figure S33. SEM image of B-(NPh_2)$_3$.

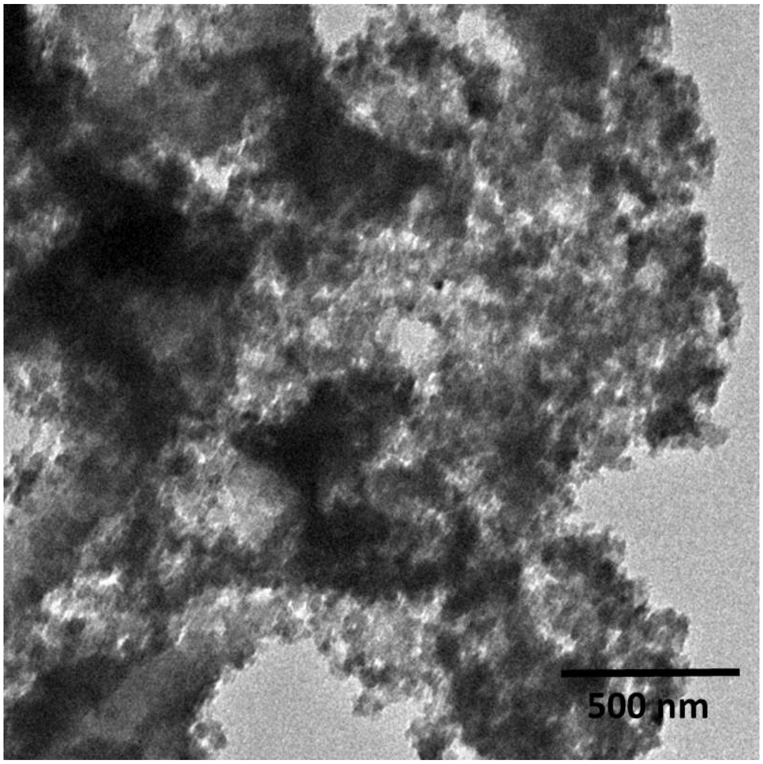

Figure S34. TEM image of B-(BOC-CB)$_3$.

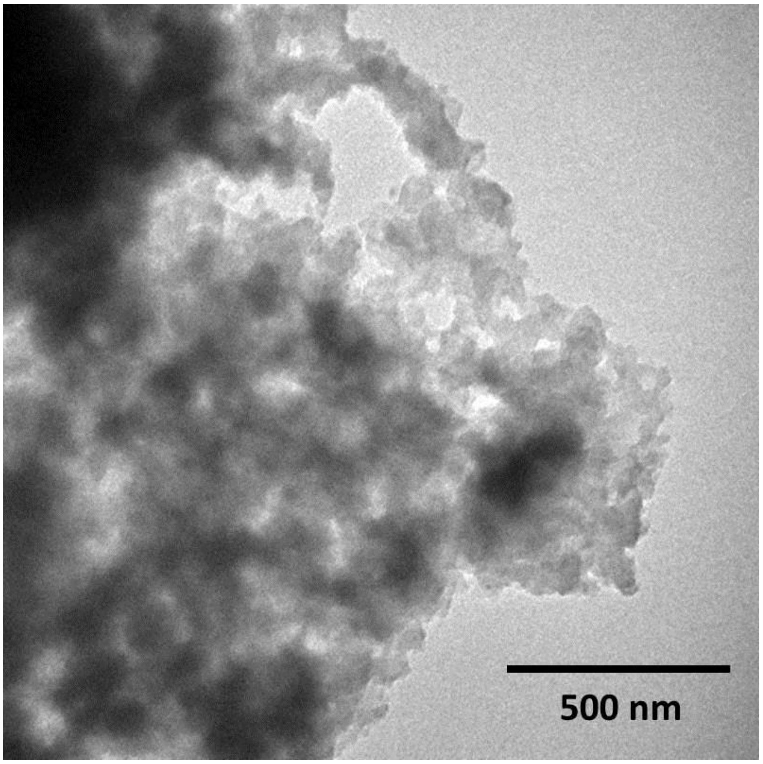

Figure S35. TEM image of B-CB$_3$.

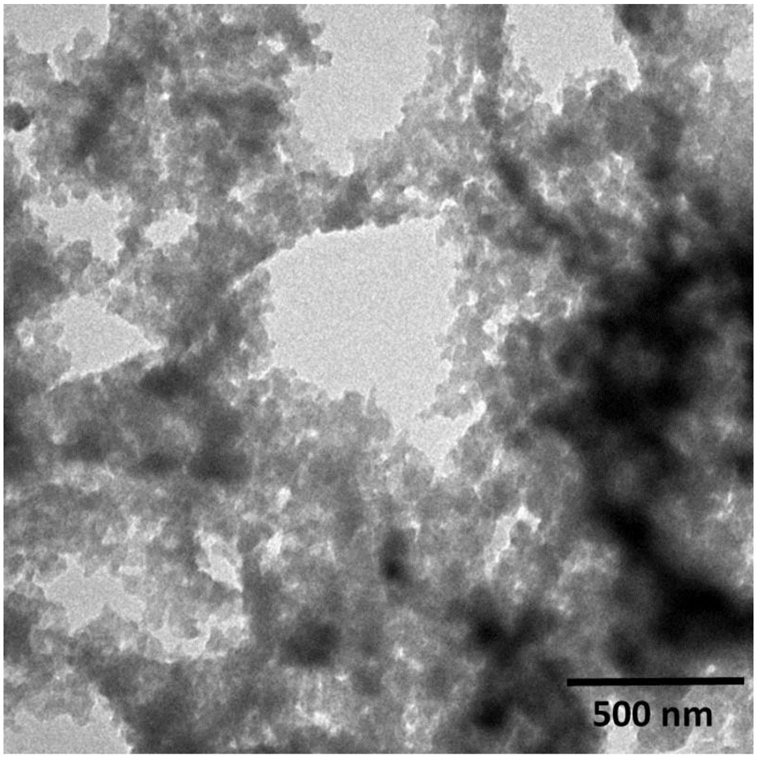

Figure S36. TEM image of B-(BOC-CB)$_2$-BT.

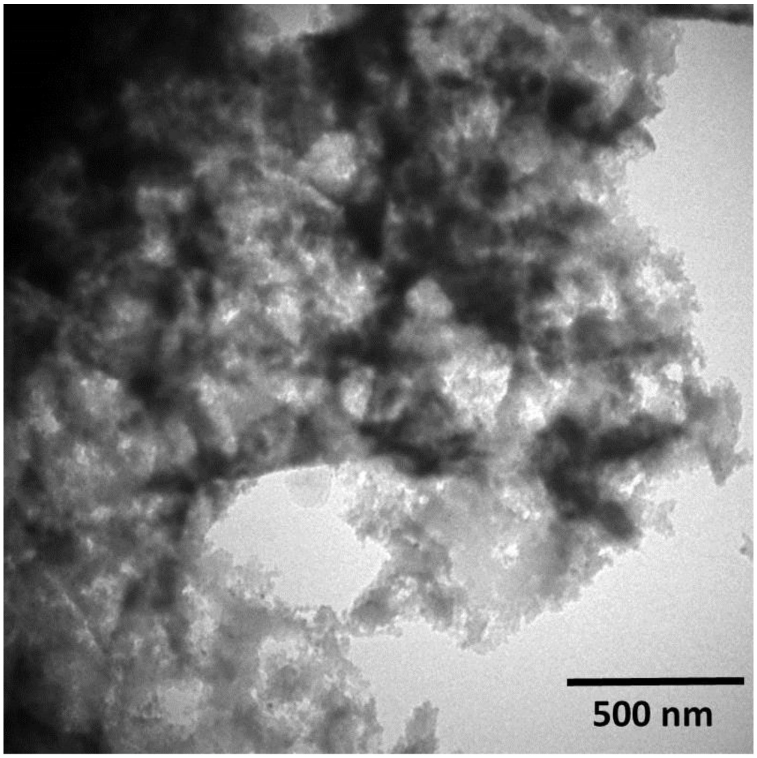

Figure S37. TEM image of B-CB$_2$-BT.